Marine Biology (2023) 170:71
https://doi.org/10.1007/s00227-023-04218-z

ORIGINAL PAPER

Effects of projected end-of-century temperature on the muscle development of neonate epaulette sharks, *Hemiscyllium ocellatum*

Peyton A. Thomas[1,6] · Emily E. Peele[1] · Carolyn R. Wheeler[2,3] · Kara Yopak[1] · Jodie L. Rummer[2,4] · John W. Mandelman[5] · Stephen T. Kinsey[1]

Received: 4 December 2022 / Accepted: 25 April 2023 / Published online: 7 May 2023

Abstract

Epaulette sharks (*Hemiscyllium ocellatum*) inhabit shallow tropical habitats with elevated and fluctuating temperatures. Yet, according to global climate change projections, water temperatures in these habitats will rise beyond current cyclical variability, warranting further studies incorporating chronically elevated temperature exposure in this species. This study examined the differences in skeletal muscle morphological and metabolic properties in neonate epaulette sharks exposed to their current-day ambient (27 °C) or projected end-of-century (31 °C) habitat temperatures throughout embryonic and neonatal development. Metrics of skeletal muscle, such as muscle fiber size and density, nuclear density, and satellite cell density, were used to assess the relative contribution of hypertrophic and hyperplastic growth processes. Capillary density was measured as a proxy for peripheral oxygen supply to muscle tissue. At 31 °C, sharks hatched earlier, but were similar in body size 60 days post-hatch. Muscle fiber size, nuclear density, and capillary density were similar between temperature regimes. However, fiber density was lower, satellite cell density was higher, and fibers associated with satellite cells were smaller in sharks reared at 31 °C. These results suggest that elevated temperature may impair or slow satellite cell fusion to existing fibers and new fiber formation. To assess potential metabolic and developmental consequences of elevated temperatures, oxidative damage (2,4-DNPH, 8-OHdG, 4-HNE), protein degradation (Ubiquitin, LC3B, Hsp70), and muscle differentiation (Myf5, Myogenin) markers were measured. Protein carbonylation was higher at elevated temperatures, suggesting that warmer incubation temperatures at early life stages may result in oxidative damage accrual. However, protein degradation and muscle differentiation markers did not differ. These results suggest that projected end-of-century temperatures may alter muscle growth and metabolism in tropical shark species with potential consequences to shark growth and fitness.

Keywords Climate change · Elasmobranch · Fish · Muscle · Temperature

Responsible Editor: S. Hamilton.

✉ Peyton A. Thomas
peyton.thomas@colorado.edu

[1] Department of Biology and Marine Biology, University of North Carolina at Wilmington, Wilmington, NC 28403, USA

[2] ARC Centre of Excellence for Coral Reef Studies, James Cook University, Townsville, QLD 4814, Australia

[3] School for the Environment, The University of Massachusetts Boston, Boston, MA 02125, USA

[4] Marine Biology, College of Science and Engineering, James Cook University, Townsville, QLD 4811, Australia

[5] Anderson Cabot Center for Ocean Life, New England Aquarium, Boston, MA 02110, USA

[6] Present Address: Institute of Arctic and Alpine Research, 4001 Discovery Drive, Boulder, CO 80303, USA

Introduction

Global sea surface temperatures have risen by 0.5 °C over the last century and continue to increase, due to anthropogenic greenhouse gas emissions (Bindoff et al. 2019; Mingle 2020; IPCC 2022). Temperature is a driving force of changes to natural environmental processes and organism geographic distribution (Hofmann and Todgham 2010; Schulte 2015; Portner 2021; Diaz-Carballido et al. 2022). Ectotherms often have optimal thermal ranges of physiological performance, defined by temperature thresholds of metabolic demand, because metabolic rate increases exponentially with acute temperature increases due to the thermodynamics of molecular interactions and cellular kinetic energy (Fry 1971; Gillooly et al. 2001; Clarke and Fraser 2004; Angilletta 2009;

Schulte et al. 2011; Zuo et al. 2012; Schulte 2015; Allen-Ankins and Stoffels 2017).

Thermal ranges of physiological performance are dependent on evolutionary and organismal thermal history, as well as ontogenetic stage (Schulte et al. 2011; Larios-Soriano et al. 2021; Portner 2021). Warm-acclimated tropical and sub-tropical ectotherms appear to have an inherent advantage over polar populations in coping with increases in environmental temperature, because they have higher thermal tolerances (Somero 2010). However, both tropical and polar organisms are conditioned to environments with greater temperature stability and may already live closer to their upper thermal tolerance limits, potentially making them more threatened by climate change than organisms from mid-latitudes (Portner and Farrell 2008; Tewksbury et al. 2008; Portner and Peck 2010; Somero 2010, 2012; Rummer et al. 2014; McDonnell and Chapman 2015; Flynn and Todgham 2018; Bennett et al. 2021). Likewise, marine ectotherms might also be more vulnerable to warming than terrestrial ectotherms due to living close to their upper thermal limits and having fewer options for thermal refugia (Pinsky et al. 2019; Vilmar and Di Santo 2022).

Physiological performance of ectotherms (such as fishes) is inherently connected to the functionality of separate, but coordinated organ and tissue systems (Johnston 2006). For example, skeletal muscle growth and function influences locomotion, overall body size, and whole organism metabolism (Johnston 1991; Sanger 1993; Syme and Shadwick 2011; Di Santo 2022; Vilmar and Di Santo 2022). Skeletal muscle may comprise up to 60% of a fish's total body mass, which is a higher percentage compared to many vertebrates, including humans, in which muscle comprises an average of 40% total body mass (Sänger and Stroiber 2001; Biressi et al. 2007; Frontera and Ochala 2015). Though resting muscle has lower metabolic activity than other vital organs, such as the heart, liver, and brain, the shear mass of skeletal muscle and the adaptive contractile responses to mechanical stimuli in fishes makes it an essential tissue to study in the context of development and metabolic maintenance under changing temperature regimes (Goldspink 1985; Sanger 1993; Johnston et al. 2011).

Skeletal muscle is highly plastic and can alter metabolic and contractile function based on the environment, functional demands, chemical signals, and neural input (Johnston et al. 2001; Nemova et al. 2016, 2021). Temperature can influence the balance of skeletal muscle growth mechanisms in fishes by altering rates of oxygen or metabolite transport and rates of biochemical processes involved in contractile function, resulting in downstream effects that are not completely understood (Rome 1995; Egginton et al. 2000; de Paula et al. 2014; Gamperl and Syme 2021). Further, acute or chronic temperature changes may alter muscle cellularity and the extent of oxidative stress experienced at a given time (Johnston et al. 2001; Almroth et al. 2015; Takata et al. 2018).

Fish skeletal muscle grows by a mix of hyperplasia and hypertrophy (Johnston et al. 2011; Priester et al. 2011). Hyperplasia is an increase in the number of muscle fibers, while hypertrophy is an increase in the size of existing muscle fibers. Muscle precursor cells, or satellite cells, fuse with existing fibers throughout muscle development, causing nuclear accretion in those existing fibers and thus, fiber hypertrophy. Satellite cells can also fuse with each other to form new myofibers and contribute to hyperplastic growth by increasing muscle fiber number (Johnston et al. 2011; Boltana et al. 2017). Thus, the satellite cell population size at any given stage may provide evidence of the trajectory and method of muscle development (Moss and Leblond 1971; Johnston et al. 1998b; Zammit et al. 2006), while nuclear density (number of nuclei per muscle fiber) is a record of past satellite cell fusion events (Kinsey et al. 2011). Assessing the functional morphology of skeletal muscle in a broad range of species may expand our understanding of sensitivity versus adaptability and how morphology relates to animal behavior or swimming performance (Johnston et al. 2001; Vilmar and Di Santo 2022). Studies on the effects of prolonged elevated temperature on fish muscle physiology and morphology at early ontogenetic stages have primarily focused on teleosts, or bony fishes (Scott and Johnston 2012; Boltana et al. 2017; Takata et al. 2018; Balbuena-Pecino et al. 2019; Coughlin et al. 2020; Lim et al. 2020). However, the impact of chronically elevated temperatures on muscle growth in elasmobranchs (Class Chondrichthyes: sharks, skates, and rays) is currently unknown.

Some studies have shown that early ontogenetic stages of elasmobranchs are particularly vulnerable to high temperatures (Rosa et al. 2014; Pouca et al. 2018; Musa et al. 2020; Santos et al. 2021). A tropical shark species, the brown-banded bamboo shark, *Chiloscyllium punctatum*, reared under a projected end-of-century temperature of 4 °C above their current daytime conditions during the embryonic life stage hatched earlier, had higher resting metabolic rates in both embryos and juveniles, decreased juvenile body condition, and showed reduced survival at 30 days post-hatch (Rosa et al. 2014). Yet, while increased temperature is expected to impact whole body condition and performance in elasmobranchs (Osgood et al. 2021; Rosa et al. 2014; Lear et al. 2019; Musa et al. 2020; Santos et al. 2021), no studies to date have evaluated the effects of chronically elevated temperature on muscle development in the early juvenile stages of an elasmobranch species.

The epaulette shark (*Hemiscyllium ocellatum*) is a tropical, benthic, oviparous elasmobranch species native to the Great Barrier Reef (GBR) (Dudgeon et al. 2019). While the species is exceedingly tolerant of daily extreme conditions, responses to chronic temperatures at the upper limits

of their thermal range are unclear (Wheeler et al. 2021, 2022). Despite this resiliency to fluctuating conditions, juveniles of this species incubated in 32 °C from egg deposition to hatching has shown significant mortality (Gervais et al. 2016). Another recent study on juvenile *H. ocellatum* (171 ± 12.6 days post-hatch) found that sharks maintained under elevated temperatures (i.e., 32 °C) were smaller, with cessation of growth occurring after 6 weeks of exposure, and mortality occurred by 80 days (Gervais et al. 2018). These results suggest that prolonged elevated temperature exposure at or near thermal limits within a juvenile life stage may affect *H. ocellatum* development later in adulthood. Wheeler et al. (2021) further addressed metabolism, growth, and whole animal physiological performance under a chronic exposure to a sublethal temperature of 31 °C during the embryonic and juvenile life stages of the epaulette shark and found that, while sharks reared under a chronic high temperature scenario did not show signs of early mortality, sharks show decreases in body size at hatching, increases in metabolic rate, and increases in recovery time from an established exercise protocol.

The effects of elevated temperatures on growth processes are particularly relevant to *H. ocellatum* because it is endemic to the GBR region, which has already warmed by almost 1 °C since 1871 and has undergone unprecedented marine heatwaves, varying in spatial scale within the past two decades (Lough et al. 2018). Four mass heatwaves spanning most of the reef system occurred within the past 7 years, ranging in duration from weeks to months, with little knowledge of the implications on elasmobranchs and other fishes (Chin et al. 2010; Babcock et al. 2019; Fordyce et al. 2019; Bernal et al. 2020). The current study examines muscle development of a subset of neonate epaulette sharks reared at the current GBR average summer sea surface temperature and a sublethal projected end-of-century GBR summer sea surface temperature from Wheeler et al (2021). The purpose of the study was to determine whether epaulette shark musculoskeletal development is adaptive to chronically elevated temperature during an early juvenile life stage.

Methods

Animal collection and dissection

Animal collection and rearing was conducted as part of the experiment in Wheeler et al (2021). Epaulette shark embryos from one breeding pair of long term captive-held sharks were reared in egg cases at the New England Aquarium's Animal Care Center (Quincy, MA, USA) from 12 ± 2 days post-deposition to 63 ± 4.3 days post-hatching at either a current GBR average temperature (27 °C; n = 6) or at an elevated temperature that is projected for this region by the Shared Socioeconomic Pathway 5 (SSP5)-8.5 end-of-century ocean warming scenario (31 °C; n = 6) (Collins et al. 2014; Wheeler et al. 2021; IPCC 2021). All eggs within the same treatment group were incubated in one 320-L aquarium system for the duration of the experiments. These experimental treatments are described in further detail by Wheeler et al. (2021). Following temperature acclimation, specimens were shipped live overnight from the New England Aquarium to the University of North Carolina Wilmington (UNCW). Animals were euthanized with 0.4 g L^{-1} tricaine methanesulfonate (MS-222; Argent Laboratories, Redmond, WA, USA) according to the ethical guidelines of the UNCW Institutional Animal Care and Use Committee (# A1718-006) and sex, body mass (g), total length (cm), and fork length (cm) were measured. Muscle tissue from the left side of each animal, collected for molecular analyses, was immediately flash-frozen in liquid nitrogen and stored at − 80 °C.

Animals were then transcardially perfused with 0.1 M phosphate buffer (PB) followed by 4% paraformaldehyde (PFA) in 0.1 M PB. For microscopic analyses, a rectangular piece of epaxial white skeletal muscle (2–3 g) was then excised from the right side of each animal from the region immediately posterior to the epaulette spot, approximately 30% of total body length from the snout, and samples were immersed in 4% PFA at 4 °C for long-term storage until use. Fixative was replaced every three months.

Cryosectioning and staining

Fixed tissue was cryoprotected in 10% sucrose for 1 h, followed by 30% sucrose for overnight infiltration. Tissue was embedded in Tissue-Tek OCT (Sakura Fintek Inc., Torrance, CA, USA) and placed in a Leica Cryocut 1800 (Leica Microsystems Inc., Bannockburn, IL, USA) for 1 h. Fixed, frozen muscle tissue was transversely sectioned at 30 µm at a temperature between − 20 and − 22 °C on slides coated in 2 g gelatin and 0.4 g chromium potassium sulfate dodecahydrate ($CrK(SO_4)_2 \cdot 12H_2O$, Fisher Scientific, Waltham, MA, USA). Sections were stored at − 20 °C for up to 2 weeks before staining.

Tissue sections were stained to label the sarcolemma to outline each fiber, capillaries, and nuclei. Tissue sections were rehydrated in SPBS for 5 min, incubated in Fluorescein labeled *Griffonia simplicifolia* lectin (GSL-1; 1:1000, Vector Laboratories, Burlingame, CA, USA), which binds sugars on capillary endothelial cells, for 90 min, and rinsed three times with SPBS for 10 min. Tissue was then incubated in Alexa Fluor 594 or 633-labeled wheat germ agglutinin (WGA; 1:125, Invitrogen, Waltham, MA, USA), which binds sugars on the sarcolemmal membrane of muscle, for 30 min. Sections were then rinsed in Sörensen's phosphate-buffered saline (SPBS) for 15 min, incubated in

4',6'-diamidino-2-phenylindole (DAPI, dilactate; 1:50,000, Invitrogen, Waltham, MA, USA), which intercalates in DNA and labels nuclei, for 5–10 min, and rinsed in SPBS for 15 min. Slides were mounted with 1:9 Tris-glycerin, cover slipped, and dried for a few hours or overnight at 4 °C in the dark (Priester et al. 2011).

Satellite cell labeling followed a protocol adapted from Dumont and Rudnicki (2017). Sections were incubated in a 0.1 M glycine solution for 5 min, then rinsed in SPBS for 5 min. Antigen retrieval was necessary for the proper detection of antibodies in fixed tissue sections. Heat-induced epitope retrieval (HIER) was used, in which slides were heated in sodium citrate buffer (10 mM sodium citrate, 0.05% Tween 20, pH 6.0) for 5 min in a microwave, cooled to room temperature for 20 min, and washed three times in phosphate-buffered saline-Tween 20 (PBS-T) for 5 min. Sections were incubated in permeabilization buffer (0.2% Triton-X 100) for 10 min and washed twice in SPBS for 5 min. Sections were incubated for 1 h in blocking buffer (5% normal mouse serum, 2% bovine serum albumin, Fisher Scientific, Waltham, MA, USA) at room temperature, followed by incubation with an Alexa Fluor 546-labeled Pax-7 primary antibody (mouse monoclonal, 1:40, Cat # sc-514352 AF546, Santa Cruz Biotechnology, Dallas, TX, USA) in blocking buffer overnight in the dark at 4 °C. Sections were rinsed three times with SPBS for 5 min, incubated in Alexa Fluor 633 WGA for 30 min, incubated in DAPI working solution for 5–7 min, and washed twice with PBS for 5 min. Slides were cover slipped with 1:9 Tris-glycerin and stored for a few hours or overnight in the dark.

Imaging and image analysis

Sections were examined using an Olympus Fluoview FV1000 laser scanning confocal microscope (Olympus, Center Valley, PA, USA) and a Leica TCS SP8 laser scanning confocal microscope (Leica Microsystems, Inc., Buffalo Grove, IL, USA). One-µm thick optical slices were collected on the 405 nm (DAPI), 488 nm (GSL), 532 nm (Pax7), and 552/638 nm (WGA) channels. Stacks of 30 images of muscle fiber cross-sections were collected and viewed with the Olympus Fluoview v1.6a software (Olympus) and LAS X software (Leica Microsystems). Images were examined for muscle fiber size and density, and densities of myonuclei, satellite cells, and capillaries using ImageJ/Fiji software (Schindelin et al. 2012).

One hundred muscle fibers were analyzed per individual shark in a set of at least five images. Therefore, approximately 600 muscle fibers were examined from the six sharks per temperature treatment. A grid was overlaid on each image with a grid point spacing that varied slightly depending on the image magnification and fiber size so that approximately the same number of fibers were analyzed per image. Fibers that contained a grid point were selected for analysis, and 20–25 fibers were analyzed per image. The following criteria were established for objectively selecting fibers: No fibers were measured at grid points along the periphery of the image, and every 5th grid point was analyzed unless (1) the grid point was in between two fibers in which the fiber to the left was chosen, (2) the grid point was in between three or four fibers in which the fiber furthest to the left or top was chosen for analysis, or (3) the fiber contained no nuclei, in which case a fiber five grid points away was analyzed. This final criterion was needed because occasionally a fiber would have no nuclei within the section, and myonuclear domain and density cannot be calculated for zeros because they incorrectly imply that there are no nuclei within the entire length of the fiber (outside of the one-µm optical section). The inclusion of fibers that lack nuclei in cross section will lead to an underestimation of nuclear density, while excluding fibers without nuclei leads to a modest overestimate of nuclear density (Kinsey, pers comm). This approach did not affect the comparison between the two treatment groups since the same rule was applied to both.

To determine satellite cell density, grid point counting was used to determine the total tissue area, and all satellite cells in the image were counted due to their relative rarity. Satellite cells were identified by the nuclear co-localization of DAPI and Pax7, a myogenic transcription factor present in both quiescent and active satellite cells (Zammit et al. 2006), and the position in relation to the sarcolemma. DAPI and Pax7-positive nuclei positioned adjacent to, but on the outside of sarcolemma (stained with WGA) were considered satellite cells. The fiber size was also measured as described above for fibers associated with satellite cells.

Myonuclear domain and nuclear density measurements

Measurements of nuclear density were adapted from Priester et al. (2011). For calculations of the number of nuclei per millimeter of fiber (X) from fiber cross-sections, the following formula was used from (Schmalbruch and Hellhammer 1977):

$$X = (NL)/(d + l) \quad (1)$$

where N is the number of myonuclei per fiber cross-section, L is the desired length of the segment to be analyzed (1000 µm as a standard), d is the thickness of the section, and l is the mean length of the nucleus. The optical thickness of each image (1 µm) was used for d, and l was calculated from longitudinal sections. From the X value, we calculated the volume of cytoplasm per myonucleus (myonuclear domain) (Y) as:

$$Y = (CL)/X) \quad (2)$$

where C is the cross-sectional area of the fiber. Nuclear density (number of nuclei per volume of fiber) was calculated as the reciprocal of the myonuclear domain ($1/Y$).

Longitudinal sections stained in the same manner as cross-sections of myofibers were used to determine the mean myonuclear length, where measurements were taken from 3 individuals of each treatment group. To measure myonuclear domain and nuclear density, 100 nuclei were measured per fish, and the average nuclear length for each treatment group was used to calculate the myonuclear domain and nuclear density as described above.

Immunoblotting

Fresh, frozen *H. ocellatum* epaxial muscle tissue was used for western blot and dot blot analyses of the stress biomarker Hsp70 (rabbit polyclonal anti-Hsp70, 1:1000, Cat # 4872, Cell Signaling Technology, Danvers, MA, USA) and markers of oxidative stress that included lipid peroxidation (anti-4-HNE, rabbit polyclonal, 1:1000, Invitrogen, Cat # MA5-27570, Waltham, MA, USA), protein carbonylation (anti-DNP, goat polyclonal, 1:2500, Cat # D9781, Sigma Aldrich, St. Louis, MO, USA), and DNA damage (anti-8-OHdG, mouse monoclonal, 1:1000, Cat # sc-393871, Santa Cruz Biotechnology, Dallas, TX, USA). To investigate protein degradation pathways, markers of the ubiquitin–proteasome system (anti-Mono- and poly-ubiquitinylation conjugates, rabbit polyclonal, 1:1000, Cat # BML-PW8810-0500, Enzo Life Sciences, Farmingdale, NY, USA) and autophagy (anti-LC3B, rabbit polyclonal, 1:1000, Cat # 2775S, Cell Signaling Technology, Danvers, MA, USA) were evaluated. Two myogenic regulatory factors that contribute to muscle differentiation, Myogenic factor 5 (anti-Myf5, mouse monoclonal, 1:1000, Cat # sc-518039, Santa Cruz Biotechnology, Dallas, TX, USA) and Myogenin (anti-Myogenin, mouse monoclonal, 1:1000, Cat # MA5-11486, Invitrogen, Waltham, MA, USA) were also assessed. Molecular techniques were adapted from Wilson et al. (2015). Muscle tissue was homogenized in a 1:5 ratio of RIPA buffer with general protease inhibitors (Santa Cruz Biotechnology, Dallas, TX, USA), sonicated on ice for 30 s, and centrifuged at 12,000 g for 10 min to retrieve the supernatants with suspended proteins. Protein concentrations of each sample were determined using the Bradford assay (Bradford and Williams 1976).

Dot blots

The dot blot protocol follows a variation of the procedure of Robinson et al. (1999). A PVDF membrane was soaked in 100% methanol for 10 min, then soaked in 4.62 mM tris-buffered saline with 0.1% Tween 20 (TBST) for 5 min. Once the membrane was dried entirely and samples were thawed to room temperature, 30 µg of each sample was blotted onto a PVDF membrane. Membranes were blocked in 10 mL 3% bovine serum albumin (BSA, Fisher Scientific, Waltham, MA, USA) for 1 h, then incubated in 10 mL 3% BSA with the appropriate amount of primary antibody (see Table 1) overnight at 4 °C. The membranes were washed four times in TBST for 5 min, then incubated in 10 mL 3% BSA with the corresponding secondary antibody (sheep anti-mouse, 1:4000, Cat # AC111P, EMD Millipore Corp, Burlington, MA, USA; mouse anti-rabbit, 1:2000, Cat # sc-2357, Santa Cruz Biotechnology, Dallas, TX, USA; rabbit-goat, 1:2000, Cat # sc-2768, Santa Cruz Biotechnology, Dallas, TX, USA) for 1 h. The membrane was washed in TBST, then incubated in a chemiluminescence solution (ECL detection solution: 50% luminol/50% peroxide, Fisher Scientific, Waltham,

Table 1 Antibodies used for microscopy and immunoblotting techniques

Antibody Name	Manufacturer	Catalog Number	Species/Clonality	Dilution Factor
Griffonia simplicifolia lectin (GSL-I)	Vector Laboratories	FL-1101	–	1:1000
Wheat Germ Agglutinin (WGA) 594	Invitrogen	W11262	–	1:125
Wheat Germ Agglutinin (WGA) 633	Invitrogen	W21404	–	1:125
DAPI, dilactate	Invitrogen	D3571	–	1:50,000
Pax7 546	Santa Cruz Biotechnology	sc-514352 AF546	Mouse monoclonal	1:40
Hsp70	Cell Signaling Technology	4872	Rabbit polyclonal	1:1000
4-HNE	Invitrogen	MA5-27570	Rabbit polyclonal	1:1000
DNP	Sigma Aldrich	D9781	Goat polyclonal	1:2500
8-OHdG	Santa Cruz Biotechnology	sc-393871	Mouse monoclonal	1:1000
Mono- and poly-ubiquitination	Enzo Life Sciences	BML-PW8810-0500	Rabbit polyclonal	1:1000
LC3B	Cell Signaling Technology	2775S	Rabbit polyclonal	1:1000
Myf5	Santa Cruz Biotechnology	sc-518039	Mouse monoclonal	1:1000
Myogenin	Invitrogen	MA5-11486	Mouse monoclonal	1:1000

MA, USA) for 5 min, then laminated in plastic wrap. The laminated membrane was placed in a BioRad XR + imager (BioRad Laboratories, Hercules, CA, USA) to obtain images of the blots. Blots were stained using Coomassie Blue R-250 (Sigma Aldrich, St. Louis, MO, USA) and dried for at least 1 h. Once dried, the blots were imaged again for the total protein expression.

Western blots

For western blotting, samples were mixed in a 1:1 ratio with 2X Laemmli buffer and heated at 100 °C for 5 min. 30 µg of a sample was loaded into each gel lane of a 10% SDS-PAGE gel in a BioRad Mini-PROTEAN vertical electrophoresis apparatus (BioRad Laboratories, Hercules, CA, USA). Gel electrophoresis was run at room temperature using a Bio-Rad Powerpac (BioRad Laboratories, Hercules, CA, USA) starting at 80 V and increasing to 120 V once the samples passed through the stacking-resolving gel interface (approximately 30 min). A PVDF membrane was incubated in 100% methanol for 10 min, then in TBST for 5 min. Once samples and protein ladder reached the bottom of the gel, the gel was placed in a transfer system with sponges, filter paper, and PVDF membrane. The transfer step was run at 4 °C on a stir plate for 1 h at 100–130 mV/h (275 mA). The membrane with the transferred ladder and protein samples was washed five times in TBST for 5 min. Following this step, methods were identical to the dot blot protocol described above beginning with the first blocking step. Images were analyzed using ImageJ/Fiji software to quantify relative protein expression (Schindelin et al. 2012).

Statistical analysis

Relationships between morphometric and morphological variables were examined to contextualize skeletal muscle growth within changes in body size. Morphometric variables are expected to covary, such as body mass and total length or body mass and fiber size (Stickland et al. 1975). We used the Shapiro–Wilk goodness-of-fit test and boxplot visualization to test for normal distribution among all measured variables. A general linear model was used to test if there was a significant relationship between the measured trait and the covariate, as well as no significant interaction between the treatment and the covariate. $P > 0.25$ was used as a threshold for excluding interaction terms. Levene's test was used to test for homogeneity of variance. When these criteria were met, we used analysis of covariance (ANCOVA) to evaluate the effects of temperature with body mass, total age (embryonic period + post-hatch age in days), or muscle fiber size as covariates. All muscle morphometric data that met assumptions was tested using body mass or total age as covariates (Online Resource 1 and Online Resource 2); however, figures only correspond to significant results of these analyses. Capillary density, satellite cell density, cross-sectional area of satellite cell-associated muscle fibers, and immunoblotting markers were evaluated using Student's T-tests. Statistical analyses were considered significant when $P < 0.05$. Statistical power ($1-\beta$) was included for analyses that resulted in near significant temperature effects, $P < 0.10$. All statistical analyses were run in the JMP Pro 16 (SAS Institute, Cary, NC, USA).

Results

Body mass and age

The 31 °C rearing temperature was associated with earlier hatching and a 25% decrease in the embryonic period (Fig. 1a, $T_{(11)} = -6.90$, $P < 0.0001$) compared to the 27 °C rearing temperature. Individual sharks reared under the elevated temperature were younger in total age due to the earlier hatching times (Fig. 1a, $T_{(11)} = -4.46$, $P = 0.001$). However, there was no significant difference in body mass (Fig. 1b, $T_{(11)} = -1.39$, $P = 0.194$) or total length (data not shown, $T_{(11)} = -1.47$, $P = 0.172$) between treatments. Total length exhibited a positive scaling relationship with body mass (Fig. 1c, Control: $y = 12.57 + 0.324x$, $r^2 = 0.94$, $P = 0.001$; Elevated: $y = 13.11 + 0.293x$, $r^2 = 0.98$, $P = 0.0001$), and there was no effect of temperature on total length with body mass as a covariate (Fig. 1c, Body Mass: $F_{(1,11)} = 207.61$, $P < 0.001$; Temperature: $F_{(1,11)} = 0.21$, $P = 0.658$), suggesting that the size metrics were not altered by the elevated temperature.

Skeletal muscle morphological features

Fiber cross-sectional area increased with body mass as expected for hypertrophic fiber growth, but there was no evidence that temperature influenced mean skeletal muscle fiber cross-sectional area, with body mass as a covariate (total age was not a significant covariate) (Fig. 2a, ANCOVA, Body Mass: $F_{(1,11)} = 15.00$, $P = 0.005$; Temperature: $F_{(1,11)} = 0.00$, $P = 0.951$; BM*Temperature: $F_{(1,11)} = 2.29$, $P = 0.169$). Mean muscle fiber density decreased with body mass, which was also as expected for hypertrophic growth, and the elevated temperature group showed a significant reduction in fiber density (Fig. 2b, ANCOVA, Body Mass: $F_{(1,11)} = 17.37$, $P = 0.002$; Temperature: $F_{(1,11)} = 5.32$, $P = 0.047$). The decrease in fiber density in sharks reared under the elevated temperature occurred despite the lack of an effect of temperature on fiber size (Fig. 2a) and may result from a narrower range of fiber sizes when compared to sharks from the control temperature group, including fewer small, recently formed fibers. Mean capillary density, an indicator of oxygen

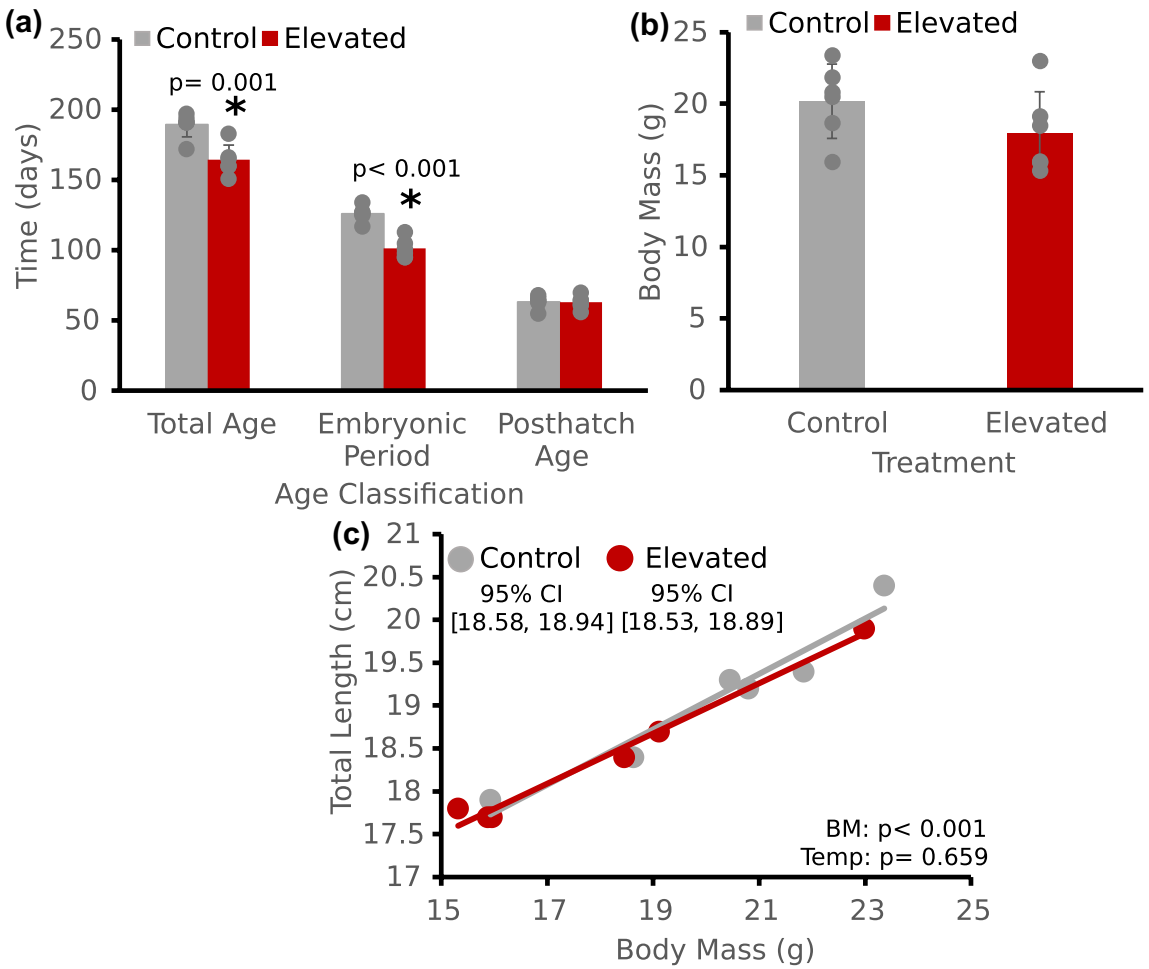

Fig. 1 **a** Total, embryonic and post-hatch age, where total age is the sum of the embryonic and post-hatch ages. **b** Body mass at the end of each temperature treatment. Embryonic period decreased under elevated temperature, which led to a decrease in total age under elevated temperature, but not a significant difference in body mass. Data in bar graphs are presented as means ± s.e.m and n = 6 animals for each temperature. An asterisk * denotes significant differences. **c** Relationship between body mass and total length for each temperature condition at the end of the temperature treatment. Data are plotted with lines fitted to each temperature group for visualization purposes, but slopes were not significantly different and ANCOVA was conducted without the temperature × covariate interaction. P-values correspond to separate effect tests from the ANCOVA model

supply, did not differ between treatments (Fig. 2c, $T_{(11)}$= 0.55, P = 0.598) and was not affected by temperature, with body mass as a covariate (ANCOVA, Body Mass: $F_{(1,11)}$= 1.51, P = 0.25; Temperature: $F_{(1,11)}$= 0.00, P = 0.986) or total age as a covariate (Fig. 2d, ANCOVA, Age: $F_{(1,11)}$= 8.62, P = 0.017; Temperature: $F_{(1,11)}$= 3.89, P = 0.08). While the temperature effect in the latter case was nearly significant, we had relatively low power to detect a difference due to limited sample availability (1 − β = 0.247).

Most muscle fibers contained a single intermyofibrillar (IM) nucleus in the middle of the fiber (Fig. 3a and b). Those containing more than one nucleus had one IM nucleus and at least one subsarcolemmal (SS) nucleus at the fiber periphery, in which the SS nucleus likely reflects a recent fusion of a satellite cell to the fiber. Myonuclear domain did not covary with body mass or total age and, while it did increase with fiber size, as is typically observed for hypertrophic fiber growth, there was no significant effect of temperature with fiber size as a covariate (Fig. 3c, ANCOVA, Fiber Cross-Sectional Area: $F_{(1,11)}$ =19.52, P = 0.002; Temperature: $F_{(1,11)}$= 0.14, P = 0.716).

Mean satellite cell density did not covary with body mass or total age and was significantly higher in sharks from the elevated temperature group (Fig. 4c, $T_{(11)}$= 5.61, P = 0.0003). Muscle fibers associated with satellite cells in sharks from the high-temperature group had a smaller mean fiber cross-sectional area (Fig. 4e, $T_{(11)}$= -3.17, P = 0.018), providing further evidence that the satellite cells from this group were associated with younger fibers.

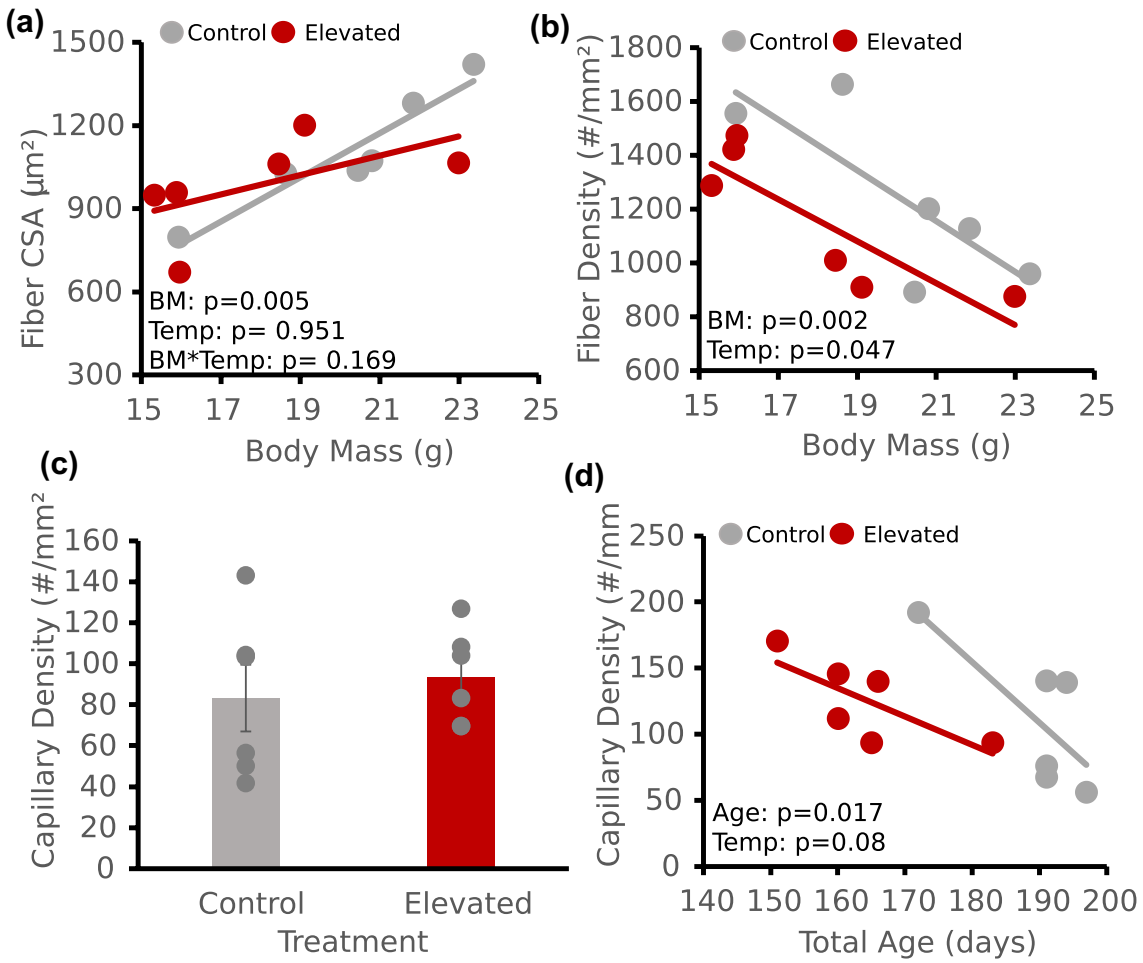

Fig. 2 Effects of temperature on **a** fiber size, **b** fiber density, and **c**, **d** capillary density. Body mass and age were included as covariates where they had a significant effect on measurements. Data are plotted with lines fitted to each temperature group in **b** and **d** for visualization purposes, but slopes were not significantly different and ANCOVA was conducted without the temperature × covariate interaction. Data are presented as mean values for each individual (n = 6 animals per treatment group and at least 100 fibers per individual). Data in bar graph are means ± s.e.m. P-values correspond to separate effect tests from the ANCOVA model

Skeletal muscle markers of oxidative stress

Dot blot results for markers of lipid peroxidation (4-HNE), DNA damage (8-OHdG), and protein carbonylation (2,4-DNPH) are shown in Fig. 5a, which revealed that mean values did not significantly differ between temperature regimes (Fig. 5b). However, total age was a significant covariate for protein carbonylation (2,4-DNPH). When total age was included as a covariate, elevated temperature led to greater protein carbonylation (Fig. 5c, Total Age: $F_{(1,11)}$= 7.29, P = 0.032; Temperature: $F_{(1,11)}$= 11.4, P = 0.009; Age*Temperature: $F_{(1,11)}$= 2.78, P = 0.134).

Skeletal muscle markers of protein degradation

Measures of protein degradation via the ubiquitin–proteasome and autophagy-lysosomal pathways were examined via dot blot for mono-and poly-conjugated ubiquitinylated proteins and western blot for lipidated LC3 (LC3B), a marker of autophagosome formation (Fig. 6a). Western blot was also used to evaluate Hsp70, which is a chaperone protein in the unfolded protein response and in the autophagy-lysosome pathway (Fig. 6a). There were no significant differences between sharks reared at control and elevated temperatures for ubiquitin (Fig. 6b, $T_{(11)}$= 1.00, P = 0.343), LC3B (Fig. 6b, $T_{(11)}$= -1.49, P = 0.183), or Hsp70 expression (Fig. 6b, $T_{(11)}$= 1.86, P = 0.092). Hsp70 was almost significantly higher in the high temperature group, but as above, a limited supply of animals yielded a relatively low statistical power (1 − β = 0.392).

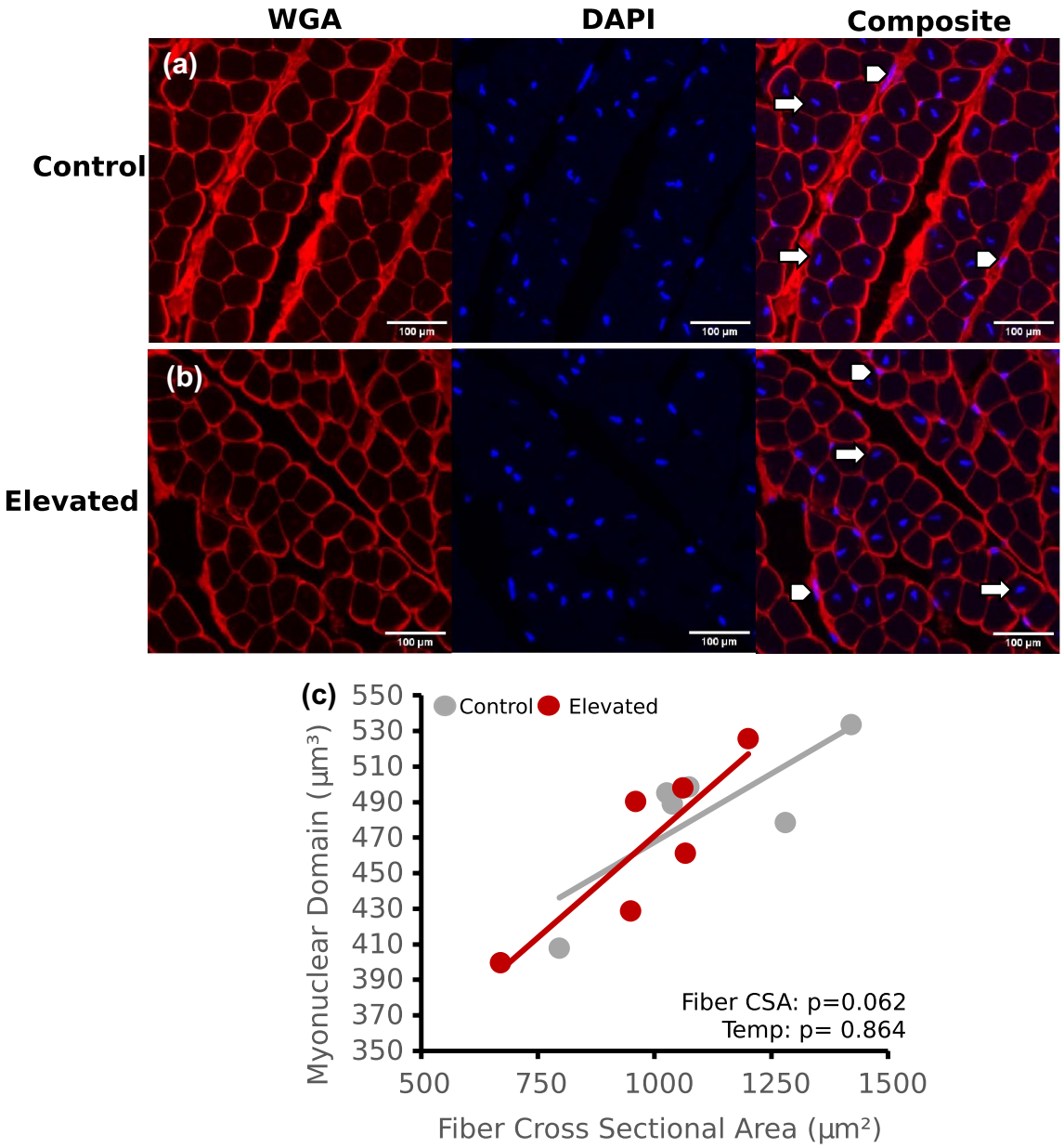

Fig. 3 Immunofluorescence showing transverse sections of epaxial muscle stained with WGA to label the sarcolemmal membrane (red) and DAPI to label nuclei (blue) for **a** control temperature and **b** elevated temperature (scale bars are 100 µm; 20X/0.3 NA, Leica SP8). White arrows indicate intermyofibrillar nuclei and white arrowheads indicate subsarcolemmal nuclei. **c** Myonuclear domain for each temperature condition with fiber cross-sectional area as a covariate. Data are plotted with lines fitted to each temperature group for visualization purposes, but slopes were not significantly different and ANCOVA was conducted without the temperature × covariate interaction. Data are presented as mean values for each individual (n = 6 animals for each temperature and at least 100 nuclei per individual). P-values correspond to separate effect tests from the ANCOVA model. Images are 500 µm × 500 µm. Scale bars are 100 µm

Skeletal muscle markers of differentiation

Markers of muscle cell differentiation were assessed via western blot (Fig. 7a). There were no effects of body mass or age on either protein, and neither Myf5 nor Myogenin mean expression differed in sharks reared under the two temperature treatments (Fig. 7b, Myf5: $T_{(11)} = 0.74$, $P = 0.480$; Myogenin: $T_{(11)} = -1.48$, $P = 0.194$).

Discussion

This study investigated whether neonate *Hemiscyllium ocellatum* reared under a 4 °C higher thermal regime, as expected from the SSP5-8.5 end-of-century ocean warming scenario, showed differences in the metabolic and structural features of skeletal muscle as compared to those reared at current-day summer temperatures. While epaulette sharks

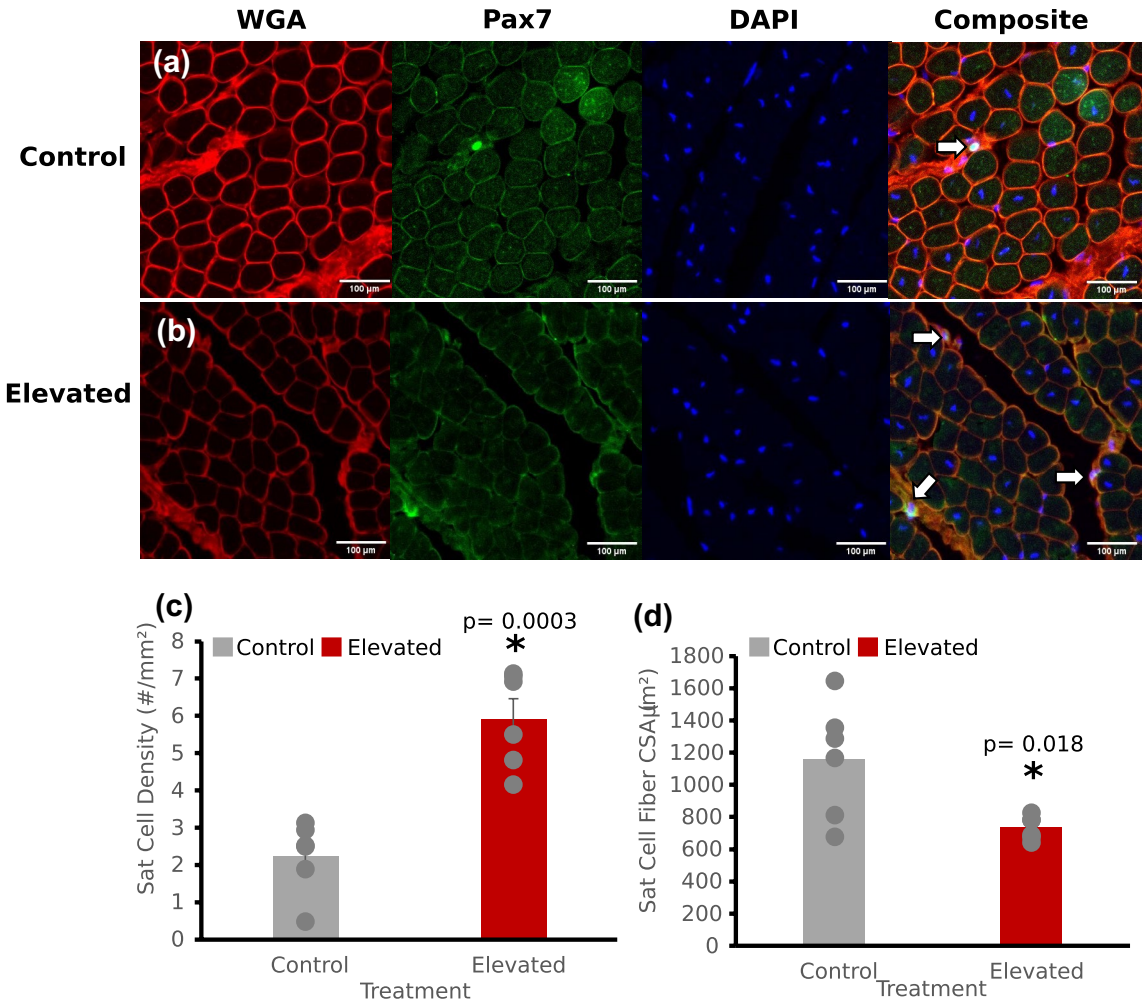

Fig. 4 Immunofluorescence showing transverse sections of epaxial muscle stained with a primary antibody for the satellite cell protein Pax7 (green), DAPI to serve as a nuclear counterstain (blue), and WGA to label the sarcolemmal membrane (red) from **a** control temperature and **b** elevated temperature (scale bars are 100 µm; 20X/0.3 NA, Leica SP8). White arrows point to satellite cells where Pax7 and nuclei are co-localized. Effect of temperature on **c** satellite cell density. and **d** cross-sectional area (CSA) of muscle fibers associated with satellite cells (n = 6 animals for each temperature and all satellite cells in an image were counted, due to their relative rarity). Data in bar graph are means ± s.e.m. and an asterisk * denotes significant differences

tolerate high temperature, high CO_2, and oxygen-limited systems, these conditions are acute and often predictable with tidal and seasonal fluctuations (Heinrich et al. 2014; Johnson et al. 2016; Gervais et al. 2018; Nay et al. 2021). When epaulette sharks were exposed to chronically elevated temperatures during their embryonic and neonatal development, they exhibited a shortened embryonic period, skeletal muscle fibers showed lower fiber density, higher satellite cell density, and increased oxidative damage to proteins compared to those reared at the current-day temperature. However, other measures of muscle structure and development did not differ between the 27 °C and 31 °C reared sharks, which might be expected for a species that inhabits fluctuating environmental conditions. The limited differences in these properties in animals reared at 31 °C may indicate a lack of muscle plasticity and an inability to acclimate, resulting in reduced aerobic scope and reduced performance (e.g., exercise protocols; Wheeler et al. 2021).

The epaulette sharks hatched earlier at 31 °C, but body size was similar to those reared at 27 °C. Shorter embryonic periods have been documented in several teleost and elasmobranch fishes when maintained at elevated temperatures within their thermal range (Gillooly et al. 2002; Schulte et al. 2011; Rosa et al. 2014; Schulte 2015). Exposure to high temperatures within an organism's thermal window during embryonic development often decreases development time by increasing rates of metabolic processes, which subsequently increases organism growth rate (Gillooly et al. 2002; Zuo et al. 2012; Rosa et al. 2014). In neonate epaulette sharks, shorter embryonic developmental time at higher

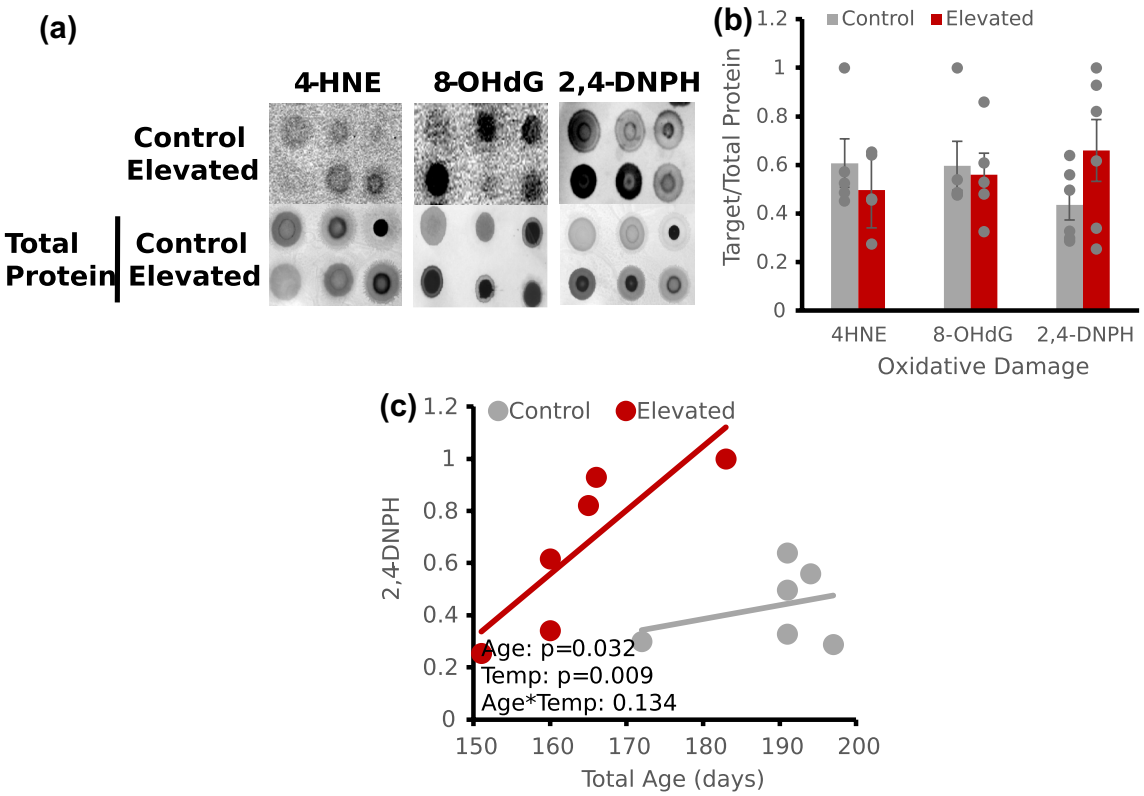

Fig. 5 **a** Dot blot images of representative samples from control and elevated temperature for markers of oxidative damage: lipid peroxidation (4-HNE), DNA damage (8-OHdG), and protein carbonylation (2,4-DNPH) in epaxial muscle. **b** Mean 4-HNE, 8-OHdG, and 2,4-DNPH levels in control (n = 6) and elevated (n = 6) temperature conditions. **c** Total age had a significant effect on 2,4-DNPH levels, and including total age as a covariate revealed a significant effect of temperature. Data in the bar graph are presented as mean ± s.e.m (n = 6 animals for each temperature) and the scatterplot is represented as mean values for each individual. P-values correspond to separate effect tests from the ANCOVA model

temperatures (up to 31 °C) is associated with increased growth rates and faster yolk consumption, with the net effect of a slightly smaller body mass at hatching (Wheeler et al. 2021). While these 31 °C hatchlings were smaller, they could have regained mass by ad libitum feeding throughout the rest of the experiments (Wheeler et al. 2021). However, at 32 °C, growth declines rapidly and mortality increases, indicating that temperatures reaching 31 °C may be the *pejus* temperature of growth in juvenile epaulettes (Gervais et al. 2016, 2018; Wheeler et al. 2021). Similar relationships between temperature and body mass are seen in other fish species, as more energy is allocated to basal metabolic energy requirements and growth, the shorter development time may lead to smaller body sizes, including into adulthood (Daufresne et al. 2009; Sheridan and Bickford 2011; Lema et al. 2019).

Thermal windows are temperature ranges set by critical thermal limits in which an organism can successfully maintain aerobic respiration; these ranges vary by ontogenetic stage and thermal history (Schulte et al. 2011; Sinclair et al. 2016; Flynn and Todgham 2018). Early ontogenetic stages tend to have narrower thermal windows, potentially from an underdeveloped capacity of cardiorespiratory systems to deal with large changes in oxygen demand (Dahlke et al. 2020; Portner 2021). Juvenile temperate fishes may have thermal windows almost half that of adults (Rombough 1997), while tropical fishes exhibit much smaller differences between embryonic, juvenile, and adult life stages, due to the comparatively narrow thermal range of their environment (Rummer et al. 2014; Sunday et al. 2019; Bennett et al. 2021). While the determination of thermal windows is set by measures of acute thermal tolerance, the crux of thermal tolerance for some species may lie in chronic temperature exposure and those carryover effects (Wheeler et al 2021, 2022). For example, seasonally acclimatized adult epaulette sharks have absolute upper thermal limits of 36–39 °C, while chronic exposure to 32 °C in juveniles may result in premature mortality (Gervais et al. 2016, 2018). These two studies, while having different thermal treatments, suggest that juvenile epaulette sharks have a lower thermal maximum than adults. However, when comparing critical thermal maxima across life stages and body sizes for wild-caught epaulette

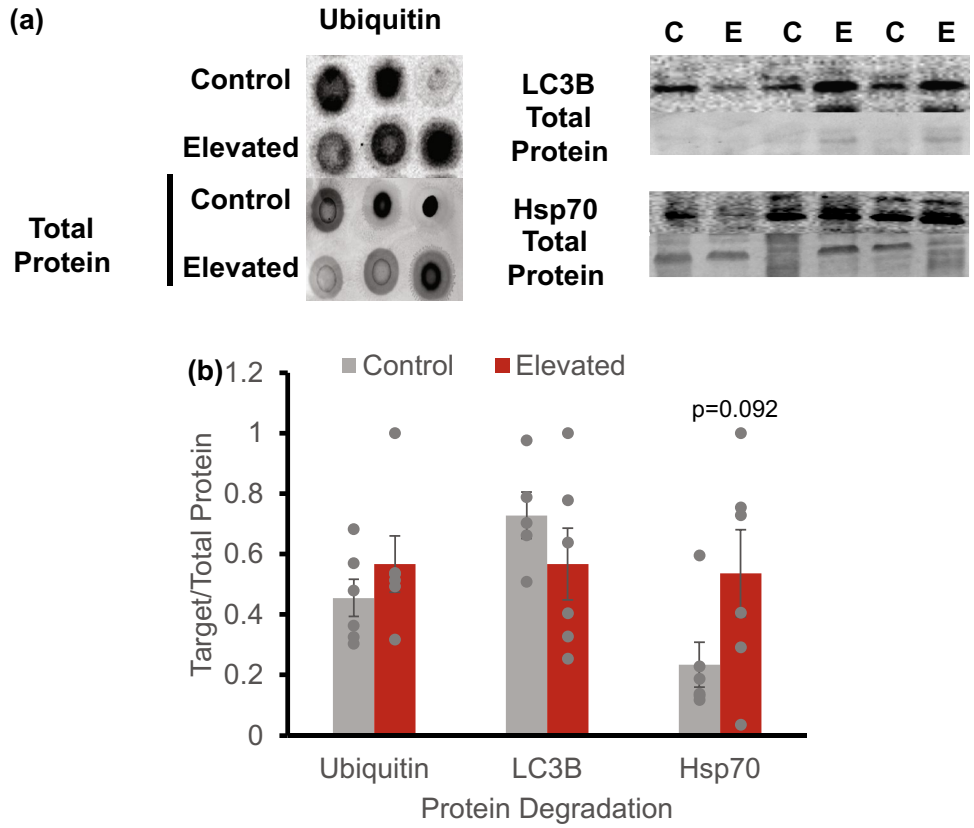

Fig. 6 **a** Dot blot and western blot images of representative samples from control and elevated temperature groups for ubiquitin (mono-and poly-conjugated ubiquitin), autophagy (LC3B), and the protein unfolding response (Hsp70) in epaxial white skeletal muscle. **b** Mean ubiquitin, LC3B, and Hsp70 expression in control and elevated temperature conditions (n = 6 animals for each temperature). Data in the bar graph are presented as mean ± s.e.m

sharks of Heron Island, GBR, with similar thermal histories, no differences were found among juveniles, subadults, and adults (Wheeler et al. 2022).

Average skeletal muscle fiber density was slightly lower in sharks from the elevated temperature. Lower fiber density would be consistent with lower muscle cellularity during early embryonic stages, and sharks from the elevated temperature had a slightly narrower fiber size distribution, including fewer small, newly formed fibers. This may explain why fiber density was lower in the elevated temperature group, but mean fiber cross-sectional area did not change. Skeletal muscle growth in early juvenile stages of teleosts is dependent on both increasing muscle fiber size via hypertrophy and increasing fiber cellularity via hyperplasia (Johnston 2006; Johnston et al. 2011). Hypertrophy constitutes the main mechanism underpinning muscle growth in many species of fish and spanning juvenile to adulthood life stages (Johnston et al. 2011). However, hyperplasia is also necessary during embryonic and juvenile life stages for species that increase body and muscle mass by several orders of magnitude throughout ontogeny (Johnston et al. 2011; Kacperczyk et al. 2011; Priester et al. 2011). Hypertrophy and hyperplasia are strongly influenced by environmental temperature, especially during embryonic development (Macqueen et al. 2008; Carey et al. 2009; Johnston et al. 2009; Scott and Johnston 2012; Ahammad et al. 2021). In this study, epaulette sharks that exhibited a lower fiber density under elevated temperatures may also be exhibiting a reduction in hyperplasia during early life stages.

Nuclear density and position influence skeletal muscle growth (Priester et al. 2011; Jimenez and Kinsey 2012). Nuclear recruitment allows for an increase in muscle fiber size, and the position of nuclei within an individual fiber determines diffusional distances for nuclear substrates and products, such as mRNA and large proteins (Priester et al. 2011; Jimenez and Kinsey 2012). The myonuclear domain describes the volume of muscle fiber that an individual nucleus controls (Koumans and Akster 1995; Priester et al. 2011). Myonuclear domain was positively correlated with body mass and fiber size for neonate epaulette sharks, which is consistent with the effects of growth seen in other vertebrates and under conditions such as aging and muscle atrophy (Van der Meer et al. 2011; Jimenez and Kinsey 2012; Hiebert and Anderson 2020). As muscle fibers grow via hypertrophy, subsarcolemmal nuclei are recruited to the fiber via satellite cell fusion, which allows muscle cells to maintain a relatively small myonuclear domain and short diffusional distances for nuclear substrates and products, thus permitting continued growth (Hall and Ralston 1989; Priester et al. 2011). While our analyses found no changes in nuclear recruitment to muscle fibers, other studies examining temperate and cold-water teleost fishes have seen an

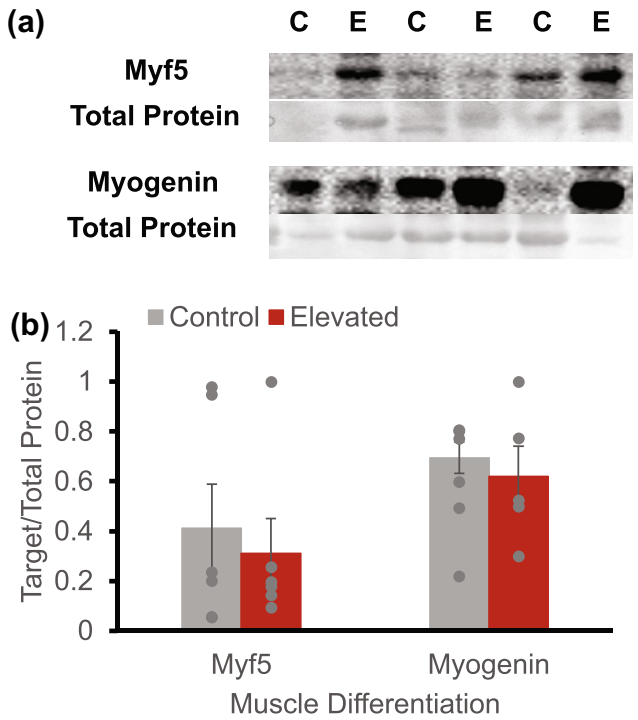

Fig. 7 **a** Western blot images of representative samples from control and elevated temperature treatments for myogenic factor 5 (Myf5) and Myogenin in epaxial muscle. **b** Mean Myf5 and Myogenin expression in control and elevated temperature conditions (n = 6 animals for each temperature). Myf5 and Myogenin were not significantly different between temperature conditions. Data are presented as mean ± s.e.m

increase in myonuclear density with elevated temperatures. When Atlantic salmon, *Salmo salar*, eggs are reared at temperatures 3–4 °C higher than their natal tributary thermal regime, fry exhibit higher nuclear densities and hypertrophic muscle growth shortly after hatching (Johnston et al. 2000). Similarly, juvenile Atlantic herring (*Clupea harengus*), juvenile pacu (*Piaractus mesopotamicus*), and larval European sea bass (*Dicentrarchus labrax*) reared under elevated temperatures exhibit higher myonuclear densities, as well as increased hypertrophic and hyperplastic growth rates (Johnston et al. 1998b; de Assis et al. 2004; Alami-Durante et al. 2006). The lack of such an effect in epaulette sharks may reflect differences in tropical species responses, especially when species are already living near their *pejus* temperatures.

Temperature can influence the timing and rate of myogenesis (Johnston et al. 1998b, 2001, 2009; Macqueen et al. 2008). Early myogenesis is a critical period for satellite cell proliferation and differentiation within an embryonic fish's dermomyotome (Steinbacher et al. 2006, 2011; Keenan and Currie 2019; Zhang et al. 2021). In the current study, satellite cell density was higher in neonate sharks reared at the elevated temperature regime, and muscle fibers associated with satellite cells were smaller in cross-sectional area. This relationship suggests that sharks maintained under the elevated temperature exhibited more satellite cells yet to fuse with existing fibers, which is supported by the smaller size of muscle fibers associated with satellite cells. This observation may be due to the shorter embryonic period observed in sharks reared under the elevated temperature regime (Zhu et al. 2014). In this case, it might be expected that the muscle fibers in sharks reared at 31 °C would have fewer nuclei (greater myonuclear domain), but this was not observed. Whether temperature effects on satellite cells are transient or influence long term muscle growth is an open question, as previous studies have shown that changes in hyperplastic growth at hatching and early juvenile stages has species-specific effects on body size and locomotory performance (Nathanailides et al. 1995; de Assis et al. 2004; Carey et al. 2009; Steinbacher et al. 2011; de la Serrana et al. 2012; Takata et al. 2018).

Animals at early juvenile stages often exhibit high metabolic rates and maintenance costs compared to adults due to constant macromolecular turnover to induce growth and rapid ontogenetic change (Monaghan et al. 2009; Metcalfe and Alonso-Alvarez 2010; Rosa et al. 2014; Boltana et al. 2017). Lipid peroxidation and DNA oxidative damage, which are both reversible processes, did not differ between the temperature groups, but protein carbonylation, which is irreversible, was higher in animals reared at the elevated temperature (Fig. 5c). While lipid peroxidation and low levels of hydrogen peroxide play an important role in promoting cell signaling, growth, resistance to oxidative stress, and increased lifespan (Wildburger et al. 2009; Milkovic et al. 2015; Else 2017), protein carbonylation is most often associated with oxidative damage and cellular dysfunction (Barreiro and Hussain 2010). Juvenile brown trout, *Salmo trutta*, and Atlantic salmon, *S. salar*, exhibit similar responses to the current observations for *H. ocellatum*, with an accumulation of damaged proteins during rapid ontogenetic growth under stressful conditions (Morgan and Metcalfe 2001; Almroth et al. 2010). While three-spined stickleback, *Gasterosteus aculeatus*, show higher oxidative DNA damage in skeletal muscle upon warm temperature acclimation during the winter breeding season (Kim et al. 2019).

Higher levels of oxidative damage may translate to greater maintenance costs (Squier 2001; Stern 2017; Neurohr et al. 2021). Hsp70 is a protein often used as an indicator of temperature stress in ectotherms, and is known to regulate the unfolded protein response, chaperone-mediated autophagy, and ubiquitin proteasome regulation (Ali et al. 2003; Madeira et al. 2016, 2018; Pan et al. 2021). However, in this study, there was no evidence of increased protein turnover in the epaulette shark via the major protein degradation pathways or in expression of Hsp70.

Climate change vulnerability will not be consistent across all organisms and individual factors may not have consistent consequences (Somero 2010; Kingsolver et al. 2013; Gunderson and Stillman 2015; Gunderson et al. 2017). The current study addressed potential climate change impacts using only temperature; yet impacts on marine organisms will more likely involve synergistic changes to temperature, dissolved oxygen, pH, salinity, and other biogeochemical and physicochemical variables (IPCC 2022). When fish muscle function is compromised by environmental stressors, such as extreme temperature, pH, oxygen, or salinity changes, this may manifest structurally as muscle atrophy, physiologically as a depression in energy metabolism, and functionally as an eventual loss of motor function from reduced muscle contraction or hyperactivity, leading to reduced swimming performance or escape responses, whole animal spasms or lack of responses to stimuli (Randall and Brauner 1991; Domenici et al. 2019; Rossi and Wright 2020; Vilmar and Di Santo 2022). Yet, often when studies assess responses to environmental variability, few encompass a combination of morphological, physiological, functional, and behavioral changes (Di Santo 2022). Likewise, many studies are based on singular acute exposures within one life stage which may not allow enough time to induce morphological adaptation. Rather, these acute responses entail balancing short-lived metabolic processes, as opposed to long-term maintenance and survival that would occur under repeated or chronic exposure throughout ontogeny leading to acclimation and eventual adaptation in structure, function, and overall behavior (Pörtner and Farrell 2008; Pörtner and Peck 2010; Somero 2012; Cook et al. 2013). The impact on an organism depends on the duration and severity of the changing variables and the species, its life history, and ontogenetic stage (Domenici et al. 2019).

This study provides the first analysis of muscle morphology and physiology of an elasmobranch species under chronic ocean warming. While this study has a number of novel components, we must acknowledge that pseudoreplication may be a factor given that all sharks originated from the same set of parents. In addition, limited sample availability led to relatively low statistical power in some cases. However, our findings related to early life temperature effects on muscle growth and oxidative damage metrics align with other studies in teleosts under a chronic exposure to upper thermal limits. Translating changes in muscle morphology to functionality is the next step in understanding potential impacts of long-term environmental variability across biological scales of locomotion and behavior. The epaulette shark may serve as a model for many other tropical, benthic elasmobranch species under a changing climate. Considering the increasing loss of marine species richness in equatorial regions as a result of ocean warming, further examination of the potential effects of both acute and chronic temperature change on the morphology, physiology, performance, and behavior of the epaulette shark and other tropical elasmobranch species is warranted.

Supplementary Information The online version contains supplementary material available at https://doi.org/10.1007/s00227-023-04218-z.

Acknowledgements The authors are grateful for the microscopy training and guidance of Dr. Carolina Priester, Mark Gay, and Dr. Alison Taylor throughout the project. The authors are also grateful for the manuscript review by Dr. Ann Pabst. We also gratefully acknowledge the UNCW Richard M. Dillaman Bioimaging facility at UNCW for access to microscopy equipment.

Author contributions All authors contributed to the study conception and design. Material preparation and data collection were performed by PT, CW, and EP. Analysis was performed by PT and SK. The first draft of the manuscript was written by PT and all authors commented on previous versions of the manuscript. All authors read and approved the final manuscript.

Funding The animal rearing was financially supported by the New England Aquarium and anonymous donors to the Anderson Cabot Center for Ocean Life. Financial support for laboratory techniques and analysis was provided by the National Institutes of Health (R15DK106688 to S.T.K.), startup funds and a UNCW College of Arts and Sciences Pilot Grant to K.E.Y., and facilities at and the University of North Carolina Wilmington.

Data availability Data are available upon request.

Declarations

Conflict of interest All authors declare that they have no affiliations with or involvement in any organization or entity with any financial interest or non-financial interest in the subject matter or materials discussed in this manuscript.

Ethical approval This study was performed in line with the principles of the Institute for Animal Care and Use Committee (IACUC). Approval was granted by IACUC of the University of North Carolina at Wilmington under IACUC A1718-006.

References

Ahammad AKS, Asaduzzaman M, Ahmed MBU, Akter S, Islam MS, Haque MM, Ceylan H, Wong LL (2021) Muscle cellularity, growth performance and growth-related gene expression of juvenile climbing perch *Anabas testudineus* in response to different eggs incubation temperature. J Therm Biol. https://doi.org/10.1016/j.jtherbio.2020.102830

Alami-Durante H, Rouel M, Kentouri M (2006) New insights into temperature-induced white muscle growth plasticity during *Dicentrarchus labrax* early life: a developmental and allometric study. Mar Biol 149:1551–1565. https://doi.org/10.1007/s00227-006-0304-6

Ali KS, Dorgai L, Gazdag A, Abraham M, Hermesz E (2003) Identification and induction of hsp70 gene by heat shock and cadmium exposure in carp. Acta Biol Hung 54:323–334. https://doi.org/10.1556/ABiol.54.2003.3-4.10

Allen-Ankins S, Stoffels RJ (2017) Contrasting fundamental and realized niches: two fishes with similar thermal performance curves

occupy different thermal habitats. Freshw Sci 36:635–652. https://doi.org/10.1086/693134
Almroth BC, Johansson A, Forlin L, Sturve J (2010) Early-age changes in oxidative stress in brown trout, *Salmo trutta*. Comp Bioch Physiol B 155:442–448. https://doi.org/10.1016/j.cbpb.2010.01.012
Almroth BC, Asker N, Wassmur B, Rosengren M, Jutfelt F, Grans A, Sundell K, Axelsson M, Sturve J (2015) Warmer water temperature results in oxidative damage in an Antarctic fish, the bald notothen. J Exp Mar Biol Ecol 468:130–137. https://doi.org/10.1016/j.jembe.2015.02.018
Angilletta MJ (2009) Thermal adaptation: a theoretical and empirical synthesis. Therm Adapt. https://doi.org/10.1093/acprof:oso/9780198570875.001.1
Babcock RC, Bustamante RH, Fulton EA, Fulton DJ, Haywood MDE, Hobday AJ, Kenyon R, Matear RJ, Plaganyi EE, Richardson AJ, Vanderklift MA (2019) Severe continental-scale impacts of climate change are happening now: extreme climate events impact marine habitat forming communities along 45% of Australia's coast. Front Mar Sci 6:14. https://doi.org/10.3389/fmars.2019.00411
Balbuena-Pecino S, Riera-Heredia N, Velez EJ, Gutierrez J, Navarro I, Riera-Codina M, Capilla E (2019) Temperature affects musculoskeletal development and muscle lipid metabolism of gilthead sea bream (*Sparus aurata*). Front Endocrinol 10:15. https://doi.org/10.3389/fendo.2019.00173
Barreiro E, Hussain SNA (2010) Protein carbonylation in skeletal muscles: impact on function. Antioxid Redox Signal 12:417–429. https://doi.org/10.1089/ars.2009.2808
Bennett JM, Sunday J, Calosi P, Villalobos F, Martinez B, Molina-Venegas R, Araujo MB, Algar AC, Clusella-Trullas S, Hawkins BA, Keith SA, Kuhn I, Rahbek C, Rodriguez L, Singer A, Morales-Castilla I, Olalla-Tarraga MA (2021) The evolution of critical thermal limits of life on Earth. Nat Commun. https://doi.org/10.1038/s41467-021-21263-8
Bernal MA, Schunter C, Lehmann R, Lightfoot DJ, Allan BJM, Veilleux HD, Rummer JL, Munday PL, Ravasi T (2020) Species-specific molecular responses of wild coral reef fishes during a marine heatwave. Sci Adv 6:11. https://doi.org/10.1126/sciadv.aay3423
Bindoff NL, Cheung WWL, Kairo JG, Arístegui J, Guinder VA, Hallberg R, Hilmi N, Jiao N, Karim MS, Levin L, O'Donoghue S, Purca Cuicapusa SR, Rinkevich B, Suga T, Tagliabue A, Williamson P (2019) Changing ocean, marine ecosystems, and dependent communities. In: Masson-Delmotte V, Zhai P, Tignor M, Poloczanska E, Mintenbeck K, Alegría A, Nicolai M, Okem A, Petzold J, Rama B, Weyer NM (eds) IPCC special report on the ocean and cryosphere in a changing climate. IPCC
Biressi S, Molinaro M, Cossu G (2007) Cellular heterogeneity during vertebrate skeletal muscle development. Dev Biol 308(3):281–293. https://doi.org/10.1016/j.ydbio.2007.06.006
Boltana S, Sanhueza N, Aguilar A, Gallardo-Escarate C, Arriagada G, Valdes JA, Soto D, Quinones RA (2017) Influences of thermal environment on fish growth. Ecol Evol 7:6814–6825. https://doi.org/10.1002/ece3.3239
Bradford MM, Williams WL (1976) New, rapid, sensitive method for protein determination. Fed Proc 35:274–274. https://doi.org/10.1006/abio.1976.9999
Carey GR, Kraft PG, Cramp RL, Franklin CE (2009) Effect of incubation temperature on muscle growth of barramundi Lates calcarifer at hatch and post-exogenous feeding. J Fish Biol 74:77–89. https://doi.org/10.1111/j.1095-8649.2008.02110.x
Chin A, Kyne PM, Walker TI, McAuley RB (2010) An integrated risk assessment for climate change: analysing the vulnerability of sharks and rays on Australia's Great Barrier Reef. Glob Change Biol 16:1936–1953. https://doi.org/10.1111/j.1365-2486.2009.02128.x
Clarke A, Fraser KPP (2004) Why does metabolism scale with temperature? Funct Ecol 18:243–251. https://doi.org/10.1111/j.0269-8463.2004.00841.x
Collins M, Knutti R, Arblaster J, Dufresne JL, Fichefet T, Friedlingstein P, Gao XJ, Gutowski WJ, Johns T, Krinner G, Shongwe M, Tebaldi C, Weaver AJ, Wehner M, Allen MR, Andrews T, Beyerle U, Bitz CM, Bony S, Booth BB, Brooks HE, Brovkin V, Browne O, Brutel-Vuilmet C, Cane M, Chadwick R, Cook E, Cook KH, Eby M, Fasullo J, Fischer EM, Forest CE, Forster P, Good P, Goosse H, Gregory JM, Hegerl GC, Hezel PJ, Hodges KI, Holland MM, Huber M, Huybrechts P, Joshi M, Kharin V, Kushnir Y, Lawrence DM, Lee RW, Liddicoat S, Lucas C, Lucht W, Marotzke J, Massonnet F, Matthews HD, Meinshausen M, Morice C, Otto A, Patricola CM, Philippon-Berthier G, Prabhat RS, Riley WJ, Rogelj J, Saenko O, Seager R, Sedlacek J, Shaffrey LC, Shindell D, Sillmann J, Slater A, Stevens B, Stott PA, Webb R, Zappa G, Zickfeld K (2014) Long-term climate change: projections, commitments and irreversibility. Clim Change 11:1029–1136
Cook DG, Iftikar FI, Baker DW, Hickey AJR, Herbert NA (2013) Low-O-2 acclimation shifts the hypoxia avoidance behaviour of snapper (Pagrus auratus) with only subtle changes in aerobic and anaerobic function. J Exp Biol 216(3):369–278. https://doi.org/10.1242/jeb.073023
Coughlin DJ, Wilson LT, Kwon ES, Travitz LS (2020) Thermal acclimation of rainbow trout myotomal muscle, can trout acclimate to a warming environment? Comp Bioch Physiol A. https://doi.org/10.1016/j.cbpa.2020.110702
Dahlke FT, Wohlrab S, Butzin M, Portner HO (2020) Thermal bottlenecks in the life cycle define climate vulnerability of fish. Science 369:65–70. https://doi.org/10.1126/science.aaz3658
Daufresne M, Lengfellner K, Sommer U (2009) Global warming benefits the small in aquatic ecosystems. Proc Natl Acad Sci USA 106:12788–12793. https://doi.org/10.1073/pnas.0902080106
de Assis JMF, Carvalho RF, Barbosa L, Agostinho CA, Dal Pal-Silva M (2004) Effects of incubation temperature on muscle morphology and growth in the pacu (*Piaractus mesopotamicus*). Aquaculture 237:251–267. https://doi.org/10.1016/j.aquaculture.2004.04.022
de Paula TG, de Almeida FLA, Carani FR, Vechetti- Júnior IJ, Padovani CR, Salomão RAS, Mareco EA, dos Santos VB, Dal-Pai-Silva M (2014) Rearing temperature induces changes in muscle growth and gene expression in juvenile pacu (*Piaractus mesopotamicus*). Comp Biochem Physiol B 169:31–37. https://doi.org/10.1016/j.cbpb.2013.12.004
de la Serrana DG, Vieira VLA, Andree KB, Darias M, Estevez A, Gisbert E, Johnston IA (2012) Development temperature has persistent effects on muscle growth responses in gilthead sea bream. PLoS ONE. https://doi.org/10.1371/journal.pone.0051884
Di Santo V (2022) EcoPhysioMechanics: Integrating Energetics and Biomechanics to Understand Fish Locomotion under Climate Change. Integr Comp Biol. https://doi.org/10.1093/icb/icac095
Diaz-Carballido PL, Mendoza-Gonzalez G, Yanez-Arenas CA, Chiappa-Carrara X (2022) Evaluation of shifts in the potential future distributions of Carcharhinid Sharks under different climate change scenarios. Front Mar Sci. https://doi.org/10.3389/fmars.2021.745501
Domenici P, Allan BJM, Lefrançois C, McCormick MI (2019) The effect of climate change on the escape kinematics and performance of fishes: implications for future predator–prey interactions. Conserv Physiol. https://doi.org/10.1093/conphys/coz078

Dudgeon CL, Corrigan S, Yang L, Allen GR, Erdmann MV, Fahmi-Sugeha HY, White WT, Naylor GJP (2019) Walking, swimming or hitching a ride? Phylogenetics and biogeography of the walking shark genus Hemiscyllium. Mar Freshw Res 71:1107–1117. https://doi.org/10.1071/MF19163

Dumont NA, Rudnicki MA (2017) Characterizing satellite cells and myogenic progenitors during skeletal muscle regeneration. In: Pellicciari C, Biggiogera M (eds) Histochemistry of single molecules: methods and protocols, 1560th edn. Springer, Dordrecht, pp 179–188. https://doi.org/10.1007/978-1-4939-6788-9_12

Egginton S, Cordiner S, Skilbeck C (2000) Thermal compensation of peripheral oxygen transport in skeletal muscle of seasonally acclimatized trout. Comp Physiol 279(2). https://doi.org/10.1152/ajpregu.2000.279.2.R375

Else PL (2017) Membrane peroxidation in vertebrates: potential role in metabolism and growth. Eur J Lipid Sci Technol 119:7. https://doi.org/10.1002/ejlt.201600319

Flynn EE, Todgham AE (2018) Thermal windows and metabolic performance curves in a developing Antarctic fish. J Comp Phys B 188:271–282. https://doi.org/10.1007/s00360-017-1124-3

Fordyce AJ, Ainsworth TA, Heron SF, Leggat W (2019) Marine heatwave hotspots in coral reef environments: physical drivers, ecophysiological outcomes, and impact upon structural complexity. Front Mar Sci 6:17. https://doi.org/10.3389/fmars.2019.00498

Frontera WR, Ochala J (2015) Skeletal muscle: a brief review of structure and function. Calcif Tissue Int 96(3):183–195. https://doi.org/10.1007/s00223-014-9915-y

Fry F (1971) The effect of environmental factors on the physiology of fish. Fish Physiol. https://doi.org/10.1016/S1546-5098(08)60146-6

Gamperl AK, Syme DA (2021) Temperature effects on the contractile performance and efficiency of oxidative muscle from a eurythermal versus a stenothermal salmonid. J Exp Biol. https://doi.org/10.1242/jeb.242487

Gervais C, Mourier J, Rummer JL (2016) Developing in warm water: irregular colouration and patterns of a neonate elasmobranch. Mar Biodivers 46:743–744. https://doi.org/10.1007/s12526-015-0429-2

Gervais CR, Nay TJ, Renshaw G, Johansen JL, Steffensen JF, Rummer JL (2018) Too hot to handle? Using movement to alleviate effects of elevated temperatures in a benthic elasmobranch, *Hemiscyllium Ocellatum*. Mar Biol 165:12. https://doi.org/10.1007/s00227-018-3427-7

Gillooly JF, Brown JH, West GB, Savage VM, Charnov EL (2001) Effects of size and temperature on metabolic rate. Science 293:2248–2251. https://doi.org/10.1126/science.1061967

Gillooly JF, Charnov EL, West GB, Savage VM, Brown JH (2002) Effects of size and temperature on developmental time. Nature 417:70–73. https://doi.org/10.1038/417070a

Goldspink G (1985) Malleability of the motor system - a comparative approach. J Exp Biol 115(1):375–391. https://doi.org/10.1242/jeb.115.1.375

Gunderson AR, Stillman JH (2015) Plasticity in thermal tolerance has limited potential to buffer ectotherms from global warming. Proc R Soc B 282:8. https://doi.org/10.1098/rspb.2015.0401

Gunderson AR, King EE, Boyer K, Tsukimura B, Stillman JH (2017) Species as stressors: heterospecific interactions and the cellular stress response under global change. Integr Comp Biol 57:90–102. https://doi.org/10.1093/icb/icx019

Hall ZW, Ralston E (1989) Nuclear domains in muscle-cells. Cell 59:771–772. https://doi.org/10.1016/0092-8674(89)90597-7

Heinrich DDU, Rummer JL, Morash AJ, Watson SA, Simpfendorfer CA, Heupel MR, Munday PL (2014) A product of its environment: the epaulette shark (*Hemiscyllium ocellatum*) exhibits physiological tolerance to elevated environmental CO2. Conserv Physiol 2:1. https://doi.org/10.1093/conphys/cou047

Hiebert A, Anderson JE (2020) Satellite cell division and fiber hypertrophy alternate with new fiber formation during indeterminate muscle growth in juvenile lake sturgeon (*Acipenser fulvescens*). Can J Zool 98:449–459. https://doi.org/10.1139/cjz-2019-0243

Hofmann GE, Todgham AE (2010) Living in the now: physiological mechanisms to tolerate a rapidly changing environment annual review of physiology. Annu Rev 75:127–145. https://doi.org/10.1146/annurev-physiol-021909-135900

IPCC (2021) Climate change 2021: the physical science basis. In: Masson-Delmotte V, Zhai P, Pirani A, Connors SL, Péan C, Berger S, Caud N, Chen Y, Goldfarb L, Gomis MI, Huang M, Leitzell K, Lonnoy E, Matthews JBR, Maycock TK, Waterfield T, Yelekçi O, Yu R, Zhou B (eds) Contribution of working group I to the sixth assessment report of the Intergovernmental Panel on Climate Change. Cambridge University Press. https://doi.org/10.1017/9781009157896

IPCC (2022) Climate change 2022: impacts, adaptation, and vulnerability. In: Pörtner DCR, Tignor M, Poloczanska ES, Mintenbeck K, Alegría A, Craig M, Langsdorf S, Löschke S, Möller V, Okem A, Rama B (eds) Working group II to the sixth assessment report of the Intergovernmental Panel on Climate Change. Cambridge University Press

Jimenez AG, Kinsey ST (2012) Nuclear DNA content variation associated with muscle fiber hypertrophic growth in fishes. J Compar Physiol B 182:531–540. https://doi.org/10.1007/s00360-011-0635-6

Johnson MS, Kraver DW, Renshaw GMC, Rummer JL (2016) Will ocean acidification affect the early ontogeny of a tropical oviparous elasmobranch (*Hemiscyllium ocellatum*)? Conserv Physiol 4:1. https://doi.org/10.1093/conphys/cow00

Johnston IA (1991) Muscle action during locomotion- a comparative perspective. J Exp Biol 160:167–185. https://doi.org/10.1242/jeb.160.1.167

Johnston IA (2006) Environment and plasticity of myogenesis in teleost fish. J Exp Biol 209(12):2249–2264. https://doi.org/10.1242/jeb.02153

Johnston IA, Cole NJ, Abercromby M, Vieira VLA (1998b) Embryonic temperature modulates muscle growth characteristics in larval and juvenile herring. J Exp Biol 201:623–646. https://doi.org/10.1242/jeb.201.5.623

Johnston IA, McLay HA, Abercromby M, Robins D (2000) Early thermal experience has different effects on growth and muscle fibre recruitment in spring- and autumn-running Atlantic salmon populations. J Exp Biol 203:2553–2564. https://doi.org/10.1242/jeb.203.17.2553

Johnston IA, Vieira VLA, Temple GK (2001) Functional consequences and population differences in the developmental plasticity of muscle to temperature in Atlantic herring *Clupea harengus*. Mar Ecol Prog Ser 213:285–300. https://doi.org/10.3354/meps213285

Johnston IA, Lee HT, Macqueen DJ, Paranthaman K, Kawashima C, Anwar A, Kinghorn JR, Dalmay T (2009) Embryonic temperature affects muscle fibre recruitment in adult zebrafish: genome-wide changes in gene and microRNA expression associated with the transition from hyperplastic to hypertrophic growth phenotypes. J Exp Biol 212:1781–1793. https://doi.org/10.1242/jeb.029918

Johnston IA, Bower NI, Macqueen DJ (2011) Growth and the regulation of myotomal muscle mass in teleost fish. J Exp Biol 214:1617–1628. https://doi.org/10.1242/jeb.038620

Kacperczyk A, Jedrzejowska I, Daczewska M (2011) Differentiation and growth of myotomal muscles in a non-model tropical fish *Pterophyllum scalare* (Teleostei: Cichlidae). Anat Histol

Embryol 40:411–418. https://doi.org/10.1111/j.1439-0264.2011.01086.x
Keenan SR, Currie PD (2019) The developmental phases of zebrafish myogenesis. J Dev Biol. https://doi.org/10.3390/jdb7020012
Kim SY, Noguera JC, Velando A (2019) Carry-over effects of early thermal conditions on somatic and germline oxidative damages are mediated by compensatory growth in sticklebacks. J Anim Ecol 88:473–483. https://doi.org/10.1111/1365-2656.12927
Kingsolver JG, Diamond SE, Buckley LB (2013) Heat stress and the fitness consequences of climate change for terrestrial ectotherms. Funct Ecol 27:1415–1423. https://doi.org/10.1111/1365-2435.12145
Kinsey ST, Locke BR, Dilliman RM (2011) Molecules in motion: influences of diffusion on metabolic structure and function in skeletal muscle. J Exp Biol 214(2):263–274. https://doi.org/10.1242/jeb.047985
Koumans JTM, Akster HA (1995) Myogenic cells in development and growth of fish. Compar Biochem Physiol A 110:3–20. https://doi.org/10.1016/0300-9629(94)00150-r
Larios-Soriano E, Re-Araujo AD, Diaz F, Lopez-Galindo LL, Rosas C, Ibarra-Castro L (2021) Effects of recent thermal history on thermal behaviour, thermal tolerance and oxygen uptake of Yellowtail Kingfish (*Seriola lalandi*) juveniles. J Therm Biol. https://doi.org/10.1016/j.jtherbio.2021.103023
Lear KO, Whitney NM, Morgan DL, Brewster LR, Whitty JM, Poulakis GR, Scharer RM, Guttridge TL, Gleiss AC (2019) Thermal performance responses in free-ranging elasmobranchs depend on habitat use and body size. Oecologia 191:829–842. https://doi.org/10.1007/s00442-019-04547-1
Lema SC, Bock SL, Malley MM, Elkins EA (2019) Warming waters beget smaller fish: evidence for reduced size and altered morphology in a desert fish following anthropogenic temperature change. Biol Lett. https://doi.org/10.1098/rsbl.2019.0518
Lim DD, Milligan CL, Morbey YE (2020) Elevated incubation temperature improves later-life swimming endurance in juvenile *Chinook salmon*, *Oncorhynchus tshawytscha*. J Fish Biol 97:1428–1439. https://doi.org/10.1111/jfb.14509
Lough JM, Anderson KD, Hughes TP (2018) Increasing thermal stress for tropical coral reefs: 1871–2017. Sci Rep 8:6079. https://doi.org/10.1038/s41598-018-24530-9
Macqueen DJ, Robb DHF, Olsen T, Melstveit L, Paxton CGM, Johnston IA (2008) Temperature until the "eyed stage" of embryogenesis programmes the growth trajectory and muscle phenotype of adult Atlantic salmon. Biol Let 4:294–298. https://doi.org/10.1098/rsbl.2007.0620
Madeira D, Costa PM, Vinagre C, Diniz MS (2016) When warming hits harder: survival, cellular stress and thermal limits of *Sparus aurata* larvae under global change. Mar Biol. https://doi.org/10.1007/s00227-016-2856-4
Madeira C, Leal MC, Diniz MS, Cabral HN, Vinagre C (2018) Thermal stress and energy metabolism in two circumtropical decapod crustaceans: responses to acute temperature events. Mar Environ Res 141:148–158. https://doi.org/10.1016/j.marenvres.2018.08.015
McDonnell LH, Chapman LJ (2015) At the edge of the thermal window: effects of elevated temperature on the resting metabolism, hypoxia tolerance and upper critical thermal limit of a widespread African cichlid. Conserv Physiol 3:13. https://doi.org/10.1093/conphys/cov050
Metcalfe NB, Alonso-Alvarez C (2010) Oxidative stress as a life-history constraint: the role of reactive oxygen species in shaping phenotypes from conception to death. Funct Ecol 24:984–996. https://doi.org/10.1111/j.1365-2435.2010.01750.x
Milkovic L, Gasparovic AC, Zarkovic N (2015) Overview on major lipid peroxidation bioactive factor 4-hydroxynonenal as pluripotent growth-regulating factor. Free Radic Res 49:850–860. https://doi.org/10.3109/10715762.2014.999056
Mingle J (2020) IPCC special report on the ocean and cryosphere in a changing climate. N Y Rev Books 67:49–51
Monaghan P, Metcalfe NB, Torres R (2009) Oxidative stress as a mediator of life history trade-offs: mechanisms, measurements and interpretation. Ecol Lett 12:75–92. https://doi.org/10.1111/j.1461-0248.2008.01258.x
Morgan IJ, Metcalfe NB (2001) Deferred costs of compensatory growth after autumnal food shortage in juvenile salmon. Proc R Soc B 268:295–301. https://doi.org/10.1098/rspb.2000.1365
Moss FP, Leblond CP (1971) Satellite cells as source of nuclei in muscles of growing rats. Anat Rec 170:421. https://doi.org/10.1002/ar.1091700405
Musa SM, Ripley DM, Moritz T, Shiels HA (2020) Ocean warming and hypoxia affect embryonic growth, fitness and survival of small-spotted catsharks, *Scyliorhinus canicula*. J Fish Biol 97:257–264. https://doi.org/10.1111/jfb.14370
Nathanailides C, Lopezalbors O, Stickland NC (1995) Influence of prehatch temperature on the development of muscle cellularity in posthatch Atlantic Salmon (*Salmo salar*). Can J Fish Aquat Sci 52:675–680. https://doi.org/10.1139/f95-068
Nay TJ, Longbottom RJ, Gervais CR, Johansen JL, Steffensen JF, Rummer JL, Hoey AS (2021) Regulate or tolerate: thermal strategy of a coral reef flat resident, the epaulette shark, Hemiscyllium ocellatum. J Fish Biol 98:723–732. https://doi.org/10.1111/jfb.14616
Nemova NN, Lysenko LA, Kantserova NP (2016) Degradation of skeletal muscle protein during growth and development of salmonid fish. Russ J Dev Biol 47:161–172. https://doi.org/10.1134/s1062360416040068
Nemova NN, Kantserova NP, Lysenko LA (2021) The traits of protein metabolism in the skeletal muscle of teleost fish. J Evol Biochem Physiol 57:626–645. https://doi.org/10.1134/s0022093021030121
Neurohr JM, Paulson ET, Kinsey ST (2021) A higher mitochondrial content is associated with greater oxidative damage, oxidative defenses, protein synthesis and ATP turnover in resting skeletal muscle. J Exp Biol 224(19). https://doi.org/10.1242/jeb.242462
Osgood GJ, White ER, Baum JK (2021) Effects of climate-change-driven gradual and acute temperature changes on shark and ray species. J Anim Ecol. https://doi.org/10.1111/1365-2656.13560
Pan Y, Zhao X, Li D, Gao TX, Song N (2021) Transcriptome analysis provides the first insight into the molecular basis of temperature plasticity in *Banggai cardinalfish*, *Pterapogon kauderni*. Compar Biochem Physiol D. https://doi.org/10.1016/j.cbd.2021.100909
Pinsky ML, Eikeset AM, McCauley DJ, Payne JL, Sunday JM (2019) Greater vulnerability to warming of marine versus terrestrial ectotherms. Nature 569:108–111. https://doi.org/10.1038/s41586-019-1132-4
Portner HO (2021) Climate impacts on organisms, ecosystems and human societies: integrating OCLTT into a wider context. J Exp Biol. https://doi.org/10.1242/jeb.238360
Portner HO, Farrell AP (2008) Ecology physiology and climate change. Science 322:690–692. https://doi.org/10.1126/science.1163156
Portner HO, Peck MA (2010) Climate change effects on fishes and fisheries: towards a cause-and-effect understanding. J Fish Biol 77:1745–1779. https://doi.org/10.1111/j.1095-8649.2010.02783.x
Pouca CV, Gervais C, Reed J, Brown C (2018) Incubation under climate warming affects behavioral lateralisation in port Jackson sharks. Symmetry (basel) 10:9. https://doi.org/10.3390/sym10060184
Priester C, Morton LC, Kinsey ST, Watanabe WO, Dillaman RM (2011) Growth patterns and nuclear distribution in white muscle fibers from black sea bass, *Centropristis striata*: evidence for the

influence of diffusion. J Exp Biol 214:1230–1239. https://doi.org/10.1242/jeb.053199
Randall D, Brauner C (1991) The effects of environmental stressors on exercise in fish. J Exp Biol 160(1):113–126. https://doi.org/10.1242/jeb.160.1.113
Robinson CE, Keshavarzian A, Pasco DS, Frommel TO, Winship DH, Holmes EW (1999) Determination of protein carbonyl groups by immunoblotting. Anal Biochem 266:48–57. https://doi.org/10.1006/abio.1998.2932
Rombough P (1997) The effects of temperature on embryonic and larval development. Global warming: implications for freshwater and marine fish. Cambridge University Press, pp 177–224. https://doi.org/10.1016/j.jtherbio.2015.03.010
Rome LC (1995) Influence of temperature on muscle properties in relation to swimming performance. Biochem Mol Biol Fishes 5:73–99. https://doi.org/10.1016/S1873-0140(06)80031-7
Rosa R, Baptista M, Lopes VM, Pegado MR, Paula JR, Trubenbach K, Leal MC, Calado R, Repolho T (2014) Early-life exposure to climate change impairs tropical shark survival. Proc R Soc B 281:7. https://doi.org/10.1098/rspb.2014.1738
Rossi GS, Wright PA (2020) Hypoxia-seeking behavior, metabolic depression and skeletal muscle function in an amphibious fish out of water. J Exp Biol 223(2):jeb213355. https://doi.org/10.1242/jeb.213355
Rummer JL, Couturier CS, Stecyk JAW, Gardiner NM, Kinch JP, Nilsson GE, Munday PL (2014) Life on the edge: thermal optima for aerobic scope of equatorial reef fishes are close to current day temperatures. Glob Change Biol 20:1055–1066. https://doi.org/10.1111/gcb.12455
Sanger AM (1993) Limits to the acclimation of fish muscle. Rev Fish Biol Fish 3(1):1–15. https://doi.org/10.1007/BF00043295
Sänger AM, Stroiber W (2001) Muscle fibre diversity and plasticity. In: Muscle growth and development. In: Johnston IA (ed) Fish physiology, 18th edn. Academic Press, San Diego, pp 187–250
Santos CP, Sampaio E, Pereira BP, Pegado MR, Borges FO, Wheeler CR, Buoyocos IA, Rummer JL, Frazão Santos C, Rosa R (2021) Elasmobranch responses to experimental warming, acidification, and oxygen loss—a meta-analysis. Front Mar Sci. https://doi.org/10.3389/fmars.2021.735377
Schindelin J, Arganda-Carreras I, Erwin Frise E, Kaynig V, Longair M, Pietzsch T, Preibisch S, Rueden C, Saalfeld S, Schmid B, Tinevez J, White DJ, Hartenstein V, Eliceiri K, Tomancak P, Cardona A (2012) Fiji: an open-source platform for biological-image analysis. Nat Methods 9:676–682
Schmalbruch H, Hellhammer U (1977) Number of nuclei in adult rat muscles with special reference to satellite cells. Anat Rec 189:169–175. https://doi.org/10.1002/ar.1091890204
Schulte PM (2015) The effects of temperature on aerobic metabolism: towards a mechanistic understanding of the responses of ectotherms to a changing environment. J Exp Biol 218:1856–1866. https://doi.org/10.1242/jeb.118851
Schulte PM, Healy TM, Fangue NA (2011) Thermal performance curves, phenotypic plasticity, and the time scales of temperature exposure. Integr Comp Biol 51:691–702. https://doi.org/10.1093/icb/icr097
Scott GR, Johnston IA (2012) Temperature during embryonic development has persistent effects on thermal acclimation capacity in zebrafish. Proc Natl Acad Sci USA 109:14247–14252. https://doi.org/10.1073/pnas.1205012109
Sheridan JA, Bickford D (2011) Shrinking body size as an ecological response to climate change. Nat Clim Chang 1:401–406. https://doi.org/10.1038/nclimate1259
Sinclair BJ, Marshall KE, Sewell MA, Levesque DL, Willett CS, Slotsbo S, Dong YW, Harley CDG, Marshall DJ, Helmuth BS, Huey RB (2016) Can we predict ectotherm responses to climate change using thermal performance curves and body temperatures? Ecol Lett 19:1372–1385. https://doi.org/10.1111/ele.12686
Somero GN (2010) The physiology of climate change: how potentials for acclimatization and genetic adaptation will determine "winners" and "losers." J Exp Biol 213:912–920. https://doi.org/10.1242/jeb.037473
Somero GN (2012) The physiology of global change: linking patterns to mechanisms. Ann Rev Mar Sci 4:39–61. https://doi.org/10.1146/annurev-marine-120710-100935
Squier TC (2001) Oxidative stress and protein aggregation during biological aging. Exp Gerontol 36:1539–1550. https://doi.org/10.1016/s0531-5565(01)00139-5
Steinbacher P, Haslett JR, Six M, Gollmann HP, Sanger AM, Stoiber W (2006) Phases of myogenic cell activation and possible role of dermomyotome cells in teleost muscle formation. Dev Dyn 235:3132–3143. https://doi.org/10.1002/dvdy.20950
Steinbacher P, Marschallinger J, Obermayer A, Neuhofer A, Sanger AM, Stoiber W (2011) Temperature-dependent modification of muscle precursor cell behaviour is an underlying reason for lasting effects on muscle cellularity and body growth of teleost fish. J Exp Biol 214:1791–1801. https://doi.org/10.1242/jeb.050096
Stern M (2017) Evidence that a mitochondrial death spiral underlies antagonistic pleiotropy. Aging Cell 16:435–443. https://doi.org/10.1111/acel.12579
Stickland NC, Widdowson EM, Goldspink G (1975) Effects of severe energy and protein deficiencies on the fibres and nuclei in skeletal muscle of pigs. Br J Nutr 34(3):421–428. https://doi.org/10.1017/s0007114575000487
Sunday J, Bennett JM, Calosi P, Clusella-Trullas S, Gravel S, Hargreaves AL, Leiva FP, Verberk W, Olalla-Tarraga MA, Morales-Castilla I (2019) Thermal tolerance patterns across latitude and elevation. Philos Trans R Soc B 374:10. https://doi.org/10.1098/rstb.2019.0036
Syme DA, Shadwick RE (2011) Red muscle function in stiff-bodied swimmers: there and almost back again. Philos Trans R Soc Lond B Biol Sci 366(1570):1507–1515. https://doi.org/10.1098/rstb.2010.0322
Takata R, Nakayama CL, Silva WDE, Bazzoli N, Luz RK (2018) The effect of water temperature on muscle cellularity and gill tissue of larval and juvenile Lophiosilurus alexandri, a neotropical freshwater fish. J Therm Biol 76:80–88. https://doi.org/10.1016/j.jtherbio.2018.07.007
Tewksbury JJ, Huey RB, Deutsch CA (2008) Ecology - Putting the heat on tropical animals. Science 320:1296–1297. https://doi.org/10.1126/science.1159328
Van der Meer SFT, Jaspers RT, Degens H (2011) Is the myonuclear domain size fixed? J Musculoskelet Neuronal Interact 11:286–297
Vilmar M, Di Santo V (2022) Swimming of sharks and rays under climate change. Rev Fish Biol Fish 32(3):765–781. https://doi.org/10.1007/s11160-022-09706-x
Wheeler CR, Rummer JL, Bailey B, Lockwood J, Vance S, Mandelman JW (2021) Future thermal regimes for epaulette sharks (*Hemiscyllium ocellatum*): growth and metabolic performance cease to be optimal. Sci Rep 11:12. https://doi.org/10.1038/s41598-020-79953-0
Wheeler CR, Lang BJ, Mandelman JW, Rummer JC (2022) The upper thermal limit of epaulette sharks (*Hemiscyllium ocellatum*) is conserved across three life history stages, sex and body size. Con Phys 10(1). https://doi.org/10.1093/conphys/coac074
Wildburger R, Mrakovcic L, Stroser M, Andrisic L, Sunjic SB, Zarkovic K, Zarkovic N (2009) Lipid peroxidation and age-associated diseases-cause or consequence? Review. Turkiye Klinikleri Tip Bilimleri Dergisi 29:189–193
Wilson WN, Baumgarner BL, Watanabe WO, Alam MS, Kinsey ST (2015) Effects of resveratrol on growth and skeletal muscle

physiology of juvenile southern flounder. Comp Biochem Physiol A 183:27–35. https://doi.org/10.1016/j.cbpa.2014.12.014

Zammit PS, Relaix F, Nagata Y, Ruiz AP, Collins CA, Partridge TA, Beauchamp JR (2006) Pax7 and myogenic progression in skeletal muscle satellite cells. J Cell Sci 119:1824–1832. https://doi.org/10.1242/jcs.02908

Zhang WY, Liu Y, Zhang H (2021) Extracellular matrix: an important regulator of cell functions and skeletal muscle development. Cell Biosci. https://doi.org/10.1186/s13578-021-00579-4

Zhu KC, Wang HL, Wang HJ, Gul Y, Yang M, Zeng C, Wang WM (2014) Characterization of muscle morphology and satellite cells, and expression of muscle-related genes in skeletal muscle of juvenile and adult *Megalobrama amblycephala*. Micron 64:66–75. https://doi.org/10.1016/j.micron.2014.03.009

Zuo WY, Moses ME, West GB, Hou C, Brown JH (2012) A general model for effects of temperature on ectotherm ontogenetic growth and development. Proc R Soc B 279:1840–1846. https://doi.org/10.1098/rspb.2011.2000